FIXED-POINT INDEX, THE INCOMPATIBILITY THEOREM, AND TORUS PARAMETRIZATION

ANDREY M. MISHCHENKO

Abstract. The fixed-point index of a homeomorphism of Jordan curves measures the number of fixed-points, with multiplicity, of the extension of the homeomorphism to the full Jordan domains in question. The now-classical Circle Index Lemma says that the fixed-point index of a positive-orientation-preserving homeomorphism of round circles is always non-negative. We begin by proving a generalization of this lemma, to accommodate Jordan curves bounding domains which do not disconnect each other. We then apply this generalization to give a new proof of Schramm's Incompatibility Theorem, which was used by Schramm to give the first proof of the rigidity of circle packings filling the complex and hyperbolic planes. As an example application, we include outlines of proofs of these circle packing theorems.

We then introduce a new tool, the so-called torus parametrization, for working with fixed-point index, which allows some problems concerning this quantity to be approached combinatorially. We apply torus parametrization to give the first purely topological proof of the following lemma: given two positively oriented Jordan curves, one may essentially prescribe the images of three points of one of the curves in the other, and obtain an orientation-preserving homeomorphism between the curves, having non-negative fixed-point index, which respects this prescription. This lemma is essential to our proof of the Incompatibility Theorem.

Contents

1. Introduction

This article is concerned with a topological quantity, the so-called *fixed-point index* of a homeomorphism of Jordan curves, which has proven useful in the study of various areas of complex analysis. We begin with its definition:

Date: April 5, 2013.

The author was partially supported by NSF grants DMS-0456940, DMS-0555750, DMS-0801029, DMS-1101373. This article is partially adapted from the Ph.D. thesis [Mis12] of the author. MSC2010 subject classification: primary: 54H25, secondary: 52C26.

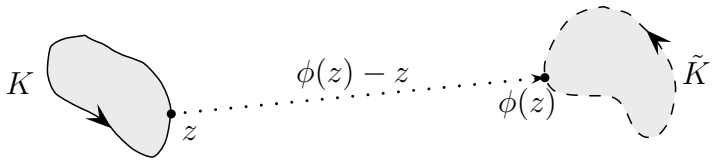

FIGURE 1. **Two closed Jordan domains K and $\tilde{K}$ so that any indexable homeomorphism $\phi : \partial K \to \partial \tilde{K}$ satisfies $\eta(\phi) = 0$.** The arrows on ∂K and $\partial \tilde{K}$ indicate the positive orientations on these Jordan curves. In this case ϕ is indexable so long as it is orientation-preserving; the fixed-point-free condition is automatic because ∂K and $\partial \tilde{K}$ do not meet. The dashed arrow represents a vector of the form $\phi(z) - z$. The vector $\phi(z) - z$ must always point "to the right," so the curve $\{\phi(z) - z\}_{z \in \partial K}$ has winding number 0 around the origin, thus $\eta(\phi) = 0$.

Definition 1.1. A *Jordan curve* is a homeomorphic image of a topological circle $\mathbb{S}^1$ in the complex plane $\mathbb{C}$. A *Jordan domain* is a bounded open set in $\mathbb{C}$ with Jordan curve boundary. We use the term *closed Jordan domain* or *compact Jordan domain* to refer to the closure of a Jordan domain. We define the *positive orientation* on a Jordan curve as usual. That is, if K is a closed Jordan domain, then as we traverse ∂K in what we call the *positive* direction, the interior of K stays to the left.

Let K and $\tilde{K}$ be closed Jordan domains. Let $\phi : \partial K \to \partial \tilde{K}$ be a homeomorphism of Jordan curves which is fixed-point-free and orientation-preserving. We call such a homeomorphism *indexable*. Then $\{\phi(z) - z\}_{z \in \partial K}$ is a closed curve in the plane which misses the origin. It has a natural orientation induced by traversing ∂K positively. Then we define the *fixed-point index* of ϕ, denoted $\eta(\phi)$, to be the winding number of $\{\phi(z) - z\}_{z \in \partial K}$ around the origin.

Two examples are shown in Figures 1 and 2. We remark that the fixed-point index depends crucially on the choice of homeomorphism, and also on the way that the sets K and $\tilde{K}$ sit on top of each other. It is a worthwhile exercise to construct an indexable homeomorphism $\partial K \to \partial \tilde{K}$, for K and $\tilde{K}$ as in Figure 2, having fixed-point index unequal to -1.

Fixed-point index has found applications for example in the theories of circle packing [HS93], Koebe uniformization [HS93], and Sierpinski carpets [Mer12, Section 12]. In all of these settings, it has been applied to prove powerful existence, rigidity, and uniformization statements. Most recently, the current author has used fixed-point index, including torus parametrization, to prove rigidity statements for collections of possibly-overlapping round disks, see [Mis12, Mis13].

The fixed-point index measures the following topological quantity: suppose that K and $\tilde{K}$ are closed Jordan domains, and $\Phi : K \to \tilde{K}$ is a homeomorphism, having finitely many fixed points, which restricts to an indexable homeomorphism $\partial\Phi : \partial K \to \partial \tilde{K}$. There is a well-understood notion of the *multiplicity* of a fixed point of Φ. Then the fixed-point index $\eta(\partial\Phi)$ counts the number of fixed-points of Φ, with multiplicity. For more discussion along these lines, see [HS93, Section 2].

In this article, we describe a new technique for working with fixed-point index, which we call the *torus parametrization* of a pair of Jordan curves, defined in Section 5. We apply torus parametrization to give a new, elementary proof of the following fundamental lemma:

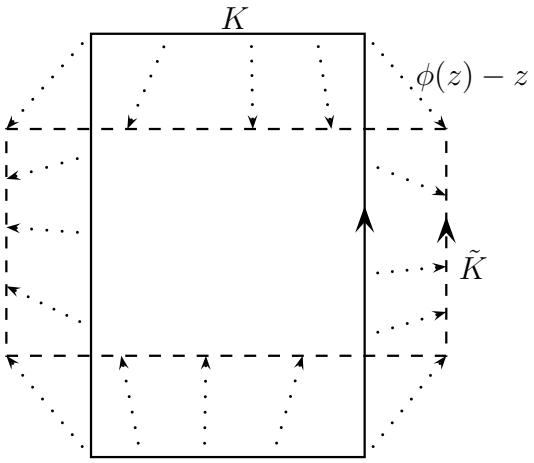

FIGURE 2. **An indexable homeomorphism $\phi : \partial K \to \partial \tilde{K}$ so that $\eta(\phi) = -1$.** Suppose we insist that ϕ identifies the respective corners as shown. Then tracing the path of the dashed vectors $\phi(z) - z$ as z traverses ∂K positively, we see that $\phi(z) - z$ winds once clockwise around the origin, thus $\eta(\phi) = -1$.

Three Point Prescription Lemma 1.2. Let K and $\tilde{K}$ be compact Jordan domains in transverse position, with boundaries oriented positively. Let $z_1, z_2, z_3 \in \partial K \setminus \partial \tilde{K}$ appear in counterclockwise order, similarly $\tilde{z}_1, \tilde{z}_2, \tilde{z}_3 \in \partial \tilde{K} \setminus \partial K$. Then there is an indexable homeomorphism $\phi : \partial K \to \partial \tilde{K}$ sending $z_i \mapsto \tilde{z}_i$ for $i = 1, 2, 3$, so that $\eta(\phi) \geq 0$.

Two Jordan domains are in *transverse position* if their boundary Jordan curves cross wherever they meet, c.f. Definition 2.3 in Section 2. The example given in Figure 2 shows that if we prescribe the images of four points, then a negative fixed-point index may be forced.

A version of the Three Point Prescription Lemma 1.2 is stated in [Ste05, Lemma 8.14], but we have not been able to fill in the details of the argument. The idea of the approach is as follows: first, any Riemann mapping $\Phi : \Omega \to \tilde{\Omega}$ between open Jordan domains extends to a homeomorphism $\partial\Phi : \partial\Omega \to \partial\tilde{\Omega}$ of their boundaries, and we may prescribe the images of three points of $\partial\Omega$ in $\partial\tilde{\Omega}$ by post-composing with self-biholomorphisms of $\tilde{\Omega}$. Next, it is known that any isolated fixed point of a holomorphic map has non-negative multiplicity, see [HS93, Section 2]. Thus the map $\partial\Phi$, if it is indexable, has non-negative fixed-point index, because the fixed-point index of $\partial\Phi$ counts the fixed points of Φ with multiplicity, completing the argument. However, it is not clear how to deal with possible fixed points in the induced boundary map $\partial\Phi$. Our proof of Lemma 1.2 uses only induction and plane topology arguments and is given in Section 6.

We also state and prove a new fundamental lemma on fixed-point index, generalizing the well-known Circle Index Lemma 2.1 which states that the fixed-point index of an indexable homeomorphism between circles is always non-negative. The Circle Index Lemma was a crucial ingredient in all of the applications of fixed-point index described above. In our generalization, round disks are replaced by closed Jordan domains which do not disconnect each other. In particular, the closed Jordan domains K and $\tilde{K}$ are said to *cut each other* if $K \setminus \tilde{K}$ or $\tilde{K} \setminus K$ is disconnected. Then:

Lemma 1.3. *Let K and $\tilde{K}$ be closed Jordan domains in transverse position, which do not cut each other, having boundaries oriented positively. Let $\phi : \partial K \to \partial \tilde{K}$ be an indexable homeomorphism. Then $\eta(\phi) \geq 0$.*

The proof appears at the end of Section 3.

As an example of the power of fixed-point index, we apply the Three Point Prescription Lemma 1.2 and Lemma 1.3 to prove a version of the Incompatibility Theorem of Schramm [Sch91, Theorem 3.1], as described in Section 3. The Incompatibility Theorem is then easily applied in Section 4 to prove some well-known rigidity theorems for circle packings. The ideas for these proofs are borrowed from [HS93; Ste05, Chapter 8].

Acknowledgments. Thanks to Jordan Watkins for many fruitful discussions, especially for pointing us strongly in the direction of what we call *torus parametrization*. Thanks also to Mario Bonk for many fruitful discussions, especially for helpful suggestions that greatly simplified the proof of Lemma 1.3.

2. Background lemmas and definitions

In the upcoming discussion it will be useful to have access to two well-known lemmas on fixed-point index. This section is devoted to introducing these two lemmas.

Our first background lemma says essentially that "the fixed-point index between two circles is always non-negative":

Circle Index Lemma 2.1. Let K and $\tilde{K}$ be closed Jordan domains in $\mathbb{C}$, with boundaries oriented positively, and let $\phi : \partial K \to \partial \tilde{K}$ be an indexable homeomorphism. Then the following hold.

(1) We have $\eta(\phi) = \eta(\phi^{-1})$.
(2) If $K \subseteq \tilde{K}$ or $\tilde{K} \subseteq K$, then $\eta(\phi) = 1$.
(3) If K and $\tilde{K}$ have disjoint interiors, then $\eta(\phi) = 0$.
(4) If ∂K and $\partial \tilde{K}$ intersect in exactly two points, then $\eta(\phi) \geq 0$.

As a consequence of the above, if K and $\tilde{K}$ are closed disks in the plane, then $\eta(\phi) \geq 0$.

Lemma 2.1 can be found in [HS93, Lemma 2.2], with a clear and complete proof. There it is indicated that a version of the lemma appeared earlier in [Str51].

The moral of our second background lemma is that fixed-point indices "add nicely":

Index Additivity Lemma 2.2. Suppose that K and L are interiorwise disjoint closed Jordan domains which meet along a single positive-length Jordan arc $\partial K \cap \partial L$, similarly for $\tilde{K}$ and $\tilde{L}$. Then $K \cup L$ and $\tilde{K} \cup \tilde{L}$ are closed Jordan domains.

Let $\phi : \partial K \to \partial \tilde{K}$ and $\psi : \partial L \to \partial \tilde{L}$ be indexable homeomorphisms. Suppose that ϕ and ψ agree on $\partial K \cap \partial L$. Let $\theta : \partial(K \cup L) \to \partial(\tilde{K} \cup \tilde{L})$ be induced via restriction to ϕ or ψ as necessary. Then θ is an indexable homeomorphism and $\eta(\theta) = \eta(\phi) + \eta(\psi)$.

Proof. The situation is as depicted in Figure 3. We may consider $\eta(\phi)$ to be $1/2\pi$ times the change in argument of the vector $\phi(z) - z$, as z traverses ∂K once in the positive direction. Then as z varies positively in ∂K and in ∂L the contributions to the sum $\eta(\phi) + \eta(\psi)$ along $\partial K \cap \partial L$ cancel. □

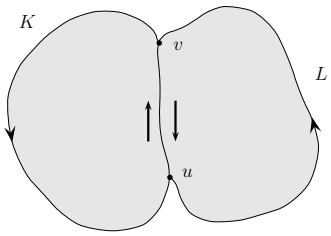

FIGURE 3. **An illustration of fixed-point index additivity.**

Next, we wish to make precise our notion of *transverse position*:

Definition 2.3. Two Jordan curves γ and $\tilde{\gamma}$ are in *transverse position* if for any point $z \in \gamma \cap \tilde{\gamma}$ where they meet, they *cross transversely*, which here means that there is an open neighborhood $U \subset \mathbb{C}$ of z and a homeomorphism $\phi : U \to \mathbb{D}$ between U and the open unit disk $\mathbb{D}$, so that $\phi(\gamma \cap U) = \mathbb{R} \cap \mathbb{D}$ and $\phi(\tilde{\gamma} \cap U) = i\mathbb{R} \cap \mathbb{D}$. Two (open or closed) Jordan domains are said to be in *transverse position* if their boundary Jordan curves are in transverse position.

Note that if two Jordan curves are in transverse position, then they meet finitely many times, by a compactness argument.

Finally, it will be helpful to have available to us the terminology of the following definition:

Definition 2.4. Suppose that $X_1, \ldots, X_n$ and $X_1', \ldots, X_n'$ are all subsets of $\mathbb{C}$. Then we say that the collections $\{X_1, \ldots, X_n\}$ and $\{X_1', \ldots, X_n'\}$ are in the same *topological configuration* if there is an orientation-preserving homeomorphism $\varphi : \mathbb{C} \to \mathbb{C}$ so that $\varphi(X_i) = X_i'$ for all $1 \leq i \leq n$. In practice the collections of objects under consideration will not be labeled X_i and X_i', but there will be some natural bijection between them. Then our requirement is that φ respects this natural bijection. We will say that certain conditions on some objects *uniquely determine* their topological configuration if any two collections of objects satisfying the given conditions are in the same topological configuration.

For example, considering a point $z \in \mathbb{C}$ and an open Jordan domain Ω, the condition that $z \in \Omega$ uniquely determines the topological configuration of $\{z, \Omega\}$, but the condition that $z \notin \Omega$ does not uniquely determine the topological configuration of $\{z, \Omega\}$. (We may have $z \in \partial\Omega$, or $z \in \mathbb{C} \setminus (\Omega \cup \partial\Omega)$, and these situations are topologically distinct.)

The following lemma says that when working with fixed-point index, we need to consider our Jordan domains only "up to topological configuration."

Lemma 2.5. *Suppose K and $\tilde{K}$ are closed Jordan domains. Let $f : \partial K \to \partial\tilde{K}$ be an indexable homeomorphism. Suppose that K' and $\tilde{K}'$ are also closed Jordan domains, so that $\{K, \tilde{K}\}$ and $\{K', \tilde{K}'\}$ are in the same topological configuration, via the homeomorphism $\varphi : \mathbb{C} \to \mathbb{C}$. Let $f' : \partial K' \to \partial\tilde{K}'$ be induced in the natural way, explicitly as $f' = \varphi|_{\partial\tilde{K}} \circ f \circ \varphi^{-1}|_{\partial K'}$. Then f' is indexable with respect to the usual orientation on $\partial K'$ and $\partial\tilde{K}'$, and $\eta(f) = \eta(f')$.*

Proof. The following is well-known. For a reference, see Chapters 1 and 2 of [FM12].

Fact 2.6. *Every orientation-preserving homeomorphism $\mathbb{C} \to \mathbb{C}$ is homotopic to the identity map via homeomorphisms.*

Thus let $H_t : \mathbb{C} \times [0,1] \to \mathbb{C}$ be such a homotopy from the identity to φ. Explicitly, for fixed t we have that H_t is an orientation-preserving homeomorphism $\mathbb{C} \to \mathbb{C}$, with H_0 equal to the identity on $\mathbb{C}$ and $H_1 = \varphi$.

Let $K_t = H_t(K)$ and $\tilde{K}_t = H_t(\tilde{K})$. Then K_t and $\tilde{K}_t$ are closed Jordan domains, because H_t is a homeomorphism. Let $f_t : \partial K_t \to \partial \tilde{K}_t$ be induced in the natural way, explicitly as $H_t|_{\partial \tilde{K}} \circ f \circ H_t^{-1}|_{\partial K_t}$. Let $\gamma_t = \{f_t(z) - z\}_{z \in \partial K_t}$. Then tautologically $\eta(f)$ is the winding number of γ_0 around the origin, and $\eta(f')$ is the winding number of γ_1 around the origin.

Every γ_t is a closed curve because ∂K_t is a closed curve and f_t is continuous. Once we establish that no γ_t passes through the origin Lemma 2.5 will be proved because we have an induced homotopy from γ_0 to γ_1, and two curves homotopic in $\mathbb{C} \setminus \{0\}$ have the same winding number around the origin. Suppose for contradiction that $0 \in \gamma_t$. Then there is a $z \in \partial K_t$ so that $f_t(z) = z$. Thus $H_t \circ f \circ H_t^{-1}(z) = z$, and so $f(H_t^{-1}(z)) = H_t^{-1}(z)$, contradicting the fixed-point-free condition on f. □

3. The Incompatibility Theorem

In this section, we state and prove the Incompatibility Theorem of Oded Schramm, appearing in [Sch91, Theorem 3.1]. Before doing so, we need some preliminary definitions:

First, a *topological rectangle* is a closed Jordan domain R with four marked points on its boundary ∂R, which we naturally call its *corners*. A *side* of R is a closed sub-arc of ∂R having two corners of R as its endpoints, and containing no other corner of R. We abuse notation slightly and use the same symbol, in this case R, to refer both to a topological rectangle and to its constituent closed Jordan domain. We define *topological triangles*, their *corners*, and their *sides* analogously, and will employ the same abuse of notation.

A *packing* of a topological rectangle R consists of a finite collection $\{K_1, \ldots, K_n\}$ of closed Jordan domains so that the following hold:

- Every K_i is contained in R.
- The K_i are pairwise interiorwise disjoint, and any two of them meet at at most one point.
- Each of the K_i meets ∂R at at most one point, and no K_i meets a corner of R.
- For every connected component U of $R \setminus \cup_{i=1}^n K_i$, we have that the closure of U is a topological triangle T each of whose sides is contained in one of the ∂K_i, or in a side of R. Then every corner of T is either a corner of R, or an intersection point of some pair of the K_i.

See Figure 4 for two examples of packings of topological rectangles. Let S_a, S_b, S_c, S_d denote the sides of R. The *contact graph* of the packing of R by $K_1, \ldots, K_n$ is the graph having vertices $v_1, \ldots, v_n$ corresponding to the $K_1, \ldots, K_n$ and v_a, v_b, v_c, v_d corresponding to the sides of R, both in the natural way, so that two distinct vertices share an edge if and only if the corresponding sets meet. Note that for example, the contact graph of a packing of a rectangle is always a triangulation of a square, that is, a triangulation of a topological closed disk having four boundary edges.

Next, suppose that we have packings of topological rectangles R and $\tilde{R}$ by collections of closed Jordan domains $K_1, \ldots, K_n$ and $\tilde{K}_1, \ldots, \tilde{K}_n$, respectively. The two packings are said to be in *transverse position* if:

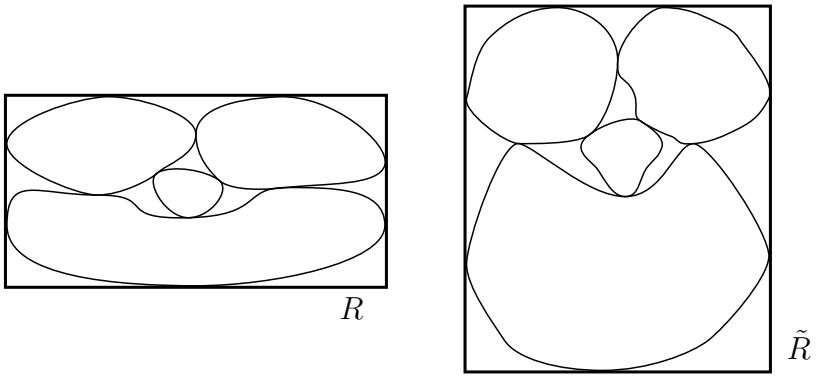

FIGURE 4. **Two topological rectangles packed with shapes.**

- For every pair of integers i and $\tilde{i}$, both between 1 and n, with possibly $i = \tilde{i}$, we have that K_i and $\tilde{K}_{\tilde{i}}$ are in transverse position as closed Jordan domains.
- For every $1 \leq i \leq n$, we have that K_i and $\tilde{R}$ are in transverse position as closed Jordan domains, as are $\tilde{K}_i$ and R.
- No intersection point of a pair of the sets $\partial K_1, \ldots, \partial K_n, \partial R$ lies on any $\partial \tilde{K}_i$ nor on $\partial \tilde{R}$. Similarly, no intersection point of a pair of the sets $\partial \tilde{K}_1, \ldots, \partial \tilde{K}_n, \partial \tilde{R}$ lies on any ∂K_i nor on ∂R.

For two examples of packings in transverse position, see Figure 6.

Finally, two closed Jordan domains K and $\tilde{K}$ which are in transverse position are said to *cut* one another if at least one of the sets $K \setminus \tilde{K}$ and $\tilde{K} \setminus K$ is disconnected. Though it is not important for us, it holds for such K and $\tilde{K}$ that $K \setminus \tilde{K}$ is connected if and only if $\tilde{K} \setminus K$ is.

We are now ready to state our version of the Incompatibility Theorem originally due to Schramm. The original appears in [Sch91, Theorem 3.1], where it is used to give the first proof of the rigidity of circle packings filling the complex plane.

When processing our statement of the Incompatibility Theorem 3.1, it may be helpful to keep the following in mind: in Schramm's original formulation, our notion of shapes *cutting one another* is referred to as *incompatibility*. Then the Incompatibility Theorem 3.1 may be remembered as, "if two incompatible rectangles are packed in the same combinatorial way, then at least one pair of corresponding shapes of the two packings will be incompatible." The precise statement given in [Sch91] is somewhat different from the one we give here. Our statement communicates the main idea of the theorem, and suffices for our applications. Our proof uses fixed-point index, with the main new tool being Lemma 1.3. The original proof by Schramm is via different methods, but is also elementary.

Incompatibility Theorem 3.1. Let R and $\tilde{R}$ be topological rectangles having sides S_a, S_b, S_c, S_d and $\tilde{S}_a, \tilde{S}_b, \tilde{S}_c, \tilde{S}_d$ respectively, in the topological configuration depicted in Figure 5. Suppose that we are given packings of R and $\tilde{R}$ by collections of closed Jordan domains $K_1, \ldots, K_n$ and $\tilde{K}_1, \ldots, \tilde{K}_n$ respectively, in transverse position, so that the packings are combinatorially equivalent in the following precise sense: denoting the contact graphs of the packings by G and $\tilde{G}$ respectively, we insist that the following holds: letting $v_a, v_b, v_c, v_d, v_1, \ldots, v_n$ and $\tilde{v}_a, \tilde{v}_b, \tilde{v}_c, \tilde{v}_d, \tilde{v}_1, \ldots, \tilde{v}_n$ denote the vertex sets of G and $\tilde{G}$ in the natural way, we have

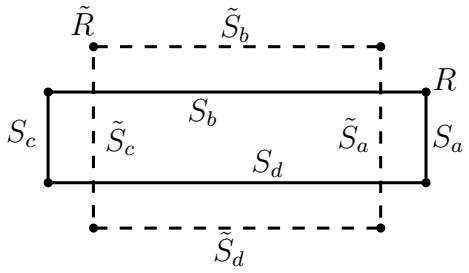

FIGURE 5

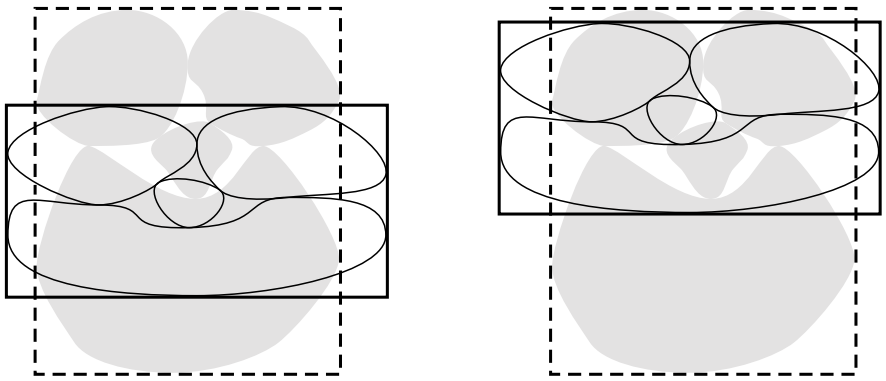

FIGURE 6. **Shapes cutting each other.** We have drawn R and $\tilde{R}$ on top of each other in two different "incompatible" ways, and in both cases some pair of corresponding shapes are "incompatible."

that G and $\tilde{G}$ are isomorphic via the identification $v_i \mapsto \tilde{v}_i$ for $i = a, b, c, d, 1, \ldots, n$. Then, there is an $1 \leq i \leq n$ so that K_i and $\tilde{K}_i$ cut each other.

For example, the packings shown in Figure 4 share a contact graph. In Figure 6 we have overlaid them in two different ways, in both cases ensuring that the hypotheses of Theorem 3.1 are satisfied. We see that in each case, a pair of corresponding closed Jordan domains cut one another.

The rest of this section consists of a proof of the Incompatibility Theorem 3.1. Our proof relies on the following simple lemma, which appeared in the introduction but is restated here for the convenience of the reader:

Lemma 1.3. *Let K and $\tilde{K}$ be closed Jordan domains in transverse position, which do not cut each other, having boundaries oriented positively. Let $\phi : \partial K \to \partial \tilde{K}$ be an indexable homeomorphism. Then $\eta(\phi) \geq 0$.*

We now give the proof of Theorem 3.1 assuming Lemma 1.3:

First, note that there is a natural bijection between the U_f and the $\tilde{U}_f$, where we write $\{U_f\}_{f \in F}$ to denote the connected components of $R \setminus \partial R \cup \bigcup_{i=1}^{n} K_i$, similarly $\{\tilde{U}_f\}_{f \in F}$. Moreover, for fixed f, we have that U_f and $\tilde{U}_f$ are topological triangles, and that the corners of U_f correspond in a natural way to those of its partner $\tilde{U}_f$. (To see this, one may consider the graphs G and $\tilde{G}$. Each is the 1-skeleton of a triangulation of a topological closed disk,

and because the graphs are isomorphic, we get that the triangulations are combinatorially equivalent. Then the U_f are in natural bijection with the faces F of this combinatorial triangulation, as are the $\tilde{U}_f$.)

Given such a pair U_f and $\tilde{U}_f$, we have that U_f and $\tilde{U}_f$ are in transverse position as closed Jordan domains, because the packings we began with are in transverse position. For every such pair U_f and $\tilde{U}_f$, orient ∂U_f and $\tilde{\partial} U_f$ positively, and let $\phi_f : \partial U_f \to \partial \tilde{U}_f$ be an indexable homeomorphism identifying corresponding corners, satisfying $\eta(\phi_f) \geq 0$. We may do so by the Three Point Prescription Lemma 1.2.

Next, for every $1 \leq i \leq n$, orienting ∂K_i and $\partial \tilde{K}_i$ positively, we obtain an indexable homeomorphism $\phi_i : \partial K_i \to \partial \tilde{K}_i$ by restriction to the ϕ_f as necessary. Also, via the same procedure, orienting ∂R and $\partial \tilde{R}$ positively, we obtain an indexable homeomorphism $\phi_R : \partial R \to \partial \tilde{R}$. Then, by the Index Additivity Lemma 2.2, we have:

$$\eta(\phi_R) = \sum_{i=1}^{n} \eta(\phi_i) + \sum_{f \in F} \eta(\phi_f)$$

Now, as we saw in Figure 2, we have that $\eta(\phi_R) = -1$. On the other hand, every $\eta(\phi_f)$ is non-negative by construction, and the $\eta(\phi_i)$ are non-negative by Lemma 1.3, which gives us a contradiction.

To complete the proof of the Incompatibility Theorem 3.1, we require the proofs of several lemmas. The proof of the Three Point Prescription Lemma 1.2 is given in Section 6 using torus parametrization. Our proof of Lemma 1.3 is inspired[1] by an argument given by Schramm in [HS93, Proof of Lemma 2.2] in support of the Circle Index Lemma 2.1. We first need to prove a topological lemma on Jordan domains which do not cut each other:

Lemma 3.2. *Suppose K and $\tilde{K}$ are closed Jordan domains in transverse position which do not cut each other, whose boundaries meet at least twice. Then the topological configuration of $\{K, \tilde{K}\}$ is determined by how many times ∂K and $\partial \tilde{K}$ meet.*

Proof. First, suppose without loss of generality that K is the closed unit disk $\bar{\mathbb{D}}$. Let $2m \geq 2$ be the number of intersection points of ∂K with $\partial \tilde{K}$. Note also that we may without loss of generality pick these arbitrarily along $\partial K = \partial \mathbb{D}$. Label these $z_1, \ldots, z_{2m}$ in clockwise order around $\partial K = \partial \mathbb{D}$. This brings us to the situation of Figure 7a.

Orient ∂K and $\partial \tilde{K}$ as usual. We now follow what happens as we traverse $\partial \tilde{K}$. By relabeling we may suppose that $\partial \tilde{K}$ enters K at z_1. Because the interior of $\tilde{K}$ stays to the left of $\partial \tilde{K}$, and because $\partial \tilde{K}$ crosses ∂K at every point where the two curves meet, it follows that $\partial \tilde{K}$ exits K at z_2. The same reasoning allows us to conclude that $\partial \tilde{K}$ enters K at z_3, etc., so we get that $\partial \tilde{K}$ enters K at z_i for all odd $1 \leq i \leq 2m$, and exits K at z_i for all even $1 \leq i \leq 2m$. This brings us to the situation of Figure 7b.

We now consider where $\partial \tilde{K}$ goes after it crosses z_1. Denote by z_i the point of $\partial K \cap \partial \tilde{K}$ at which it arrives immediately after crossing z_1, noting that then i is even. We wish to establish that then $i = 2$, so suppose for contradiction that $i \neq 2$. This brings us to the situation of Figure 7c. Then $[z_1 \to z_i]_{\partial \tilde{K}}$ disconnects $K = \bar{\mathbb{D}}$ into two components, call them A_1 and A_2. We have that every connected component of $K \setminus \tilde{K}$ must then be completely

[1] Thanks to Mario Bonk for suggesting this line of proof, greatly simplifying the required arguments.

contained in one of A_1 and A_2. But $K \setminus \tilde{K}$ is connected by hypothesis, so one of A_1 and A_2 must be disjoint from $K \setminus \tilde{K}$. We then get a contradiction, because, keeping careful track of the orientation of $\partial\tilde{K}$, we see that there are points of $K \setminus \tilde{K}$ immediately counterclockwise from z_1 along ∂K, and points of $K \setminus \tilde{K}$ immediately clockwise from z_2 along ∂K, and these lie in different components of $K \setminus [z_1 \to z_i]_{\partial\tilde{K}}$ unless $i = 2$. The same reasoning allows us to conclude that, for any odd $1 \leq j \leq 2m$, after entering K at z_j, the curve $\partial\tilde{K}$ exits K at z_{j+1}, bringing us to the situation of Figure 7d.

By the same reasoning as in the previous paragraph, we get that, for any even $1 \leq j \leq 2m$, after exiting K at z_j, the curve $\partial\tilde{K}$ enters K at z_{j+1}, adopting the convention that $z_{2m+1} = z_1$. However, in this case, there are two ways to connect z_j to z_{j+1}: roughly speaking, we may either travel clockwise around the complement of $K = \bar{\mathbb{D}}$ from z_j to z_{j+1}, or counterclockwise. If we connect every such pair z_j and z_{j+1} with "clockwise" arcs, then the resulting orientation on $\partial\tilde{K}$ is not positive with respect to the Jordan domain it bounds, see Figure 7e. Thus suppose without loss of generality, by relabeling if necessary, that z_m and z_1 are connected with a "counterclockwise" arc. Now for the remaining pairs z_j, z_{j+1}, with j even, there are no choices (up to topological equivalence) about how to draw the connecting sub-arcs of $\partial\tilde{K}$ between them, and we arrive at the situation of Figure 7f. □

Remark 3.3. Which *a priori* topological configurations can occur for two Jordan curves in transverse position is a poorly understood question, and is known as the study of *meanders*. We are fortunate that our setting is nice enough that a statement like that of Lemma 3.2 is possible. Thanks to Thomas Lam for informing us of the topic of meander theory.

Proof of Lemma 1.3. In light of Lemmas 2.5 and 3.2, we may suppose that K and $\tilde{K}$ are as in Figure 8, of course drawn with the correct number of meeting points between ∂K and $\partial\tilde{K}$. Recalling that $\eta(f)$ counts the winding number of the vector $f(z) - z$ around the origin, we consider when it is possible for $f(z) - z$ to be a positive real number. If z does not lie on the intersection of the left side of the rectangle ∂K with the interior of $\tilde{K}$, then $f(z) - z$ certainly has either a negative real component, or a non-zero imaginary component. Thus pick a z lying in this intersection. Then only way for $f(z) - z$ to be real and positive is for $f(z)$ to lie on the semicircular sub-arc of $\partial\tilde{K}$ to the right of z, as in the figure. But then, considering the orientations on ∂K and $\partial\tilde{K}$, we get that the vector $f(z) - z$ must always be turning counterclockwise at such a z, as we traverse ∂K in the positive direction. We conclude that whenever the curve $\{f(z) - z\}_{\partial K}$ crosses the positive real axis, it does so in the positive direction, thus the winding number of this curve around the origin is non-negative. □

Remark 3.4. The same Figure 8 can be used to show that under the hypotheses of Lemma 1.3, we get that $\eta(f) \leq 2$. Thus the only fixed-point indices which can be achieved in this setting are $0, 1, 2$, and all three of these occur. We do not use these facts, so working out the details is left as an exercise for the interested reader.

4. Proof of rigidity and uniformization of circle packings

As an example of the power of fixed-point index, in this section we prove three rigidity and uniformization theorems on circle packings. Theorem 4.1 is usually credited to Koebe

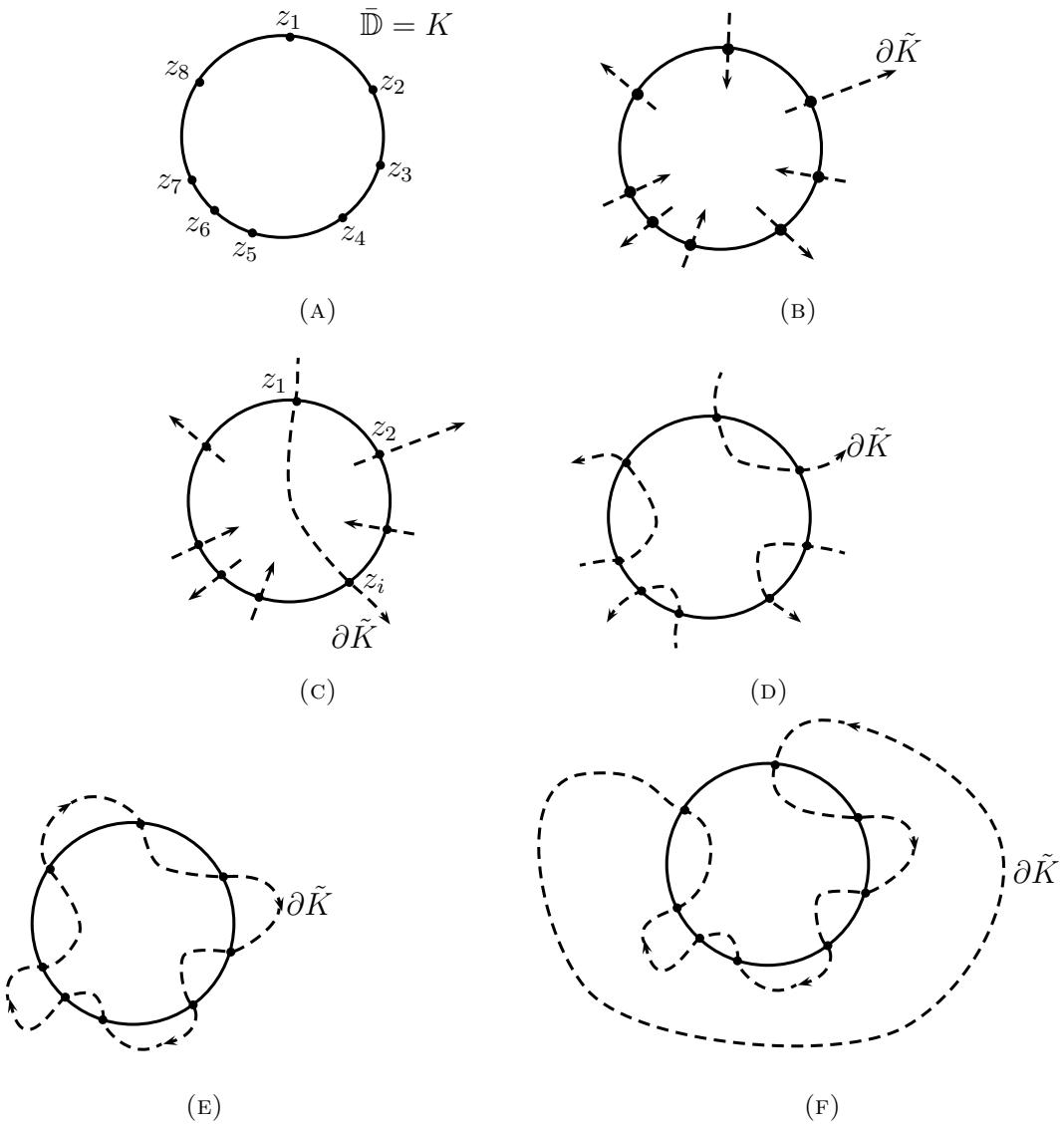

FIGURE 7. **The construction of the topologically unique pair K and $\tilde{K}$ of transversely positioned closed Jordan domains, not cutting each other, having boundaries meeting at 8 points.** The orientation on $\partial K = \partial\mathbb{D}$ is the usual, positive one, that is, the counterclockwise one. In all cases, dashed arcs are sub-arcs of $\partial\tilde{K}$.

[Koe36], Andreev [And70], and Thurston[2]. All of their proofs were via methods different from ours. Theorems 4.2 and 4.3 are originally due to Schramm [Sch91, Rigidity Theorems 1.1, 5.1], who proved them essentially via the Incompatibility Theorem 3.1, although his proof of the Incompatibility Theorem is not via fixed-point index techniques. The first ones to study circle packings by fixed-point index techniques were He and Schramm in [HS93], although they did not proceed via the Incompatibility Theorem, instead applying other normalizations

[2]Originally at his talk at the International Congress of Mathematicians, Helsinki, 1978, according to [Sac94, p. 135]. See also [Thu80, Chapter 13].

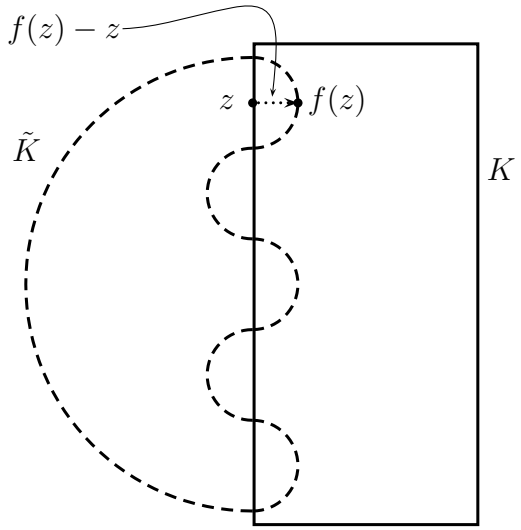

FIGURE 8. We see that whenever $f(z) - z$ is positive and real, as we traverse ∂K and $\partial \tilde{K}$ positively, the point $f(z)$ is moving upward, and the point z is moving downward, so the vector $f(z) - z$ is winding counterclockwise, thus in the positive direction.

to the packings in question, to similarly argue by contradiction. For further references on circle packing, see for example the articles [Sac94, Roh11] and their bibliographies.

We begin with some basic definitions. A *circle packing* is a collection $\mathcal{P} = \{D_i\}$ of pairwise interiorwise disjoint round closed disks in the Riemann sphere $\hat{\mathbb{C}}$. The *contact graph* of a circle packing is the graph having a vertex for every disk of the packing, so that two vertices share an edge if and only if the corresponding disks meet. Then the following hold:

Theorem 4.1. *Suppose that $\mathcal{P}$ and $\tilde{\mathcal{P}}$ are circle packings in $\hat{\mathbb{C}}$, sharing a contact graph that triangulates the 2-sphere $\mathbb{S}^2$. Then $\mathcal{P}$ and $\tilde{\mathcal{P}}$ differ by a Möbius or anti-Möbius transformation.*

Theorem 4.2. *Suppose that $\mathcal{P}$ and $\tilde{\mathcal{P}}$ are circle packings which are locally finite in $\mathbb{C}$, sharing a contact graph that triangulates a topological open disk. Then $\mathcal{P}$ and $\tilde{\mathcal{P}}$ differ by a Euclidean similarity.*

Theorem 4.3. *There cannot be two circle packings $\mathcal{P}$ and $\tilde{\mathcal{P}}$ sharing a contact graph triangulating a topological open disk, so that one is locally finite in $\mathbb{C}$ and the other is locally finite in the hyperbolic plane $\mathbb{H}^2$, equivalently the open unit disk $\mathbb{D}$.*

The rest of this section consists of the proofs of these three theorems. Before moving on, we make one note:

Remark 4.4. The statement for locally finite packings in the hyperbolic plane $\mathbb{H}^2 \cong \mathbb{D}$ analogous to Theorem 4.2 also holds. However, to apply our techniques to prove it, one would need to show that two combinatorially equivalent packings, both locally finite in $\mathbb{H}^2$, having contact graphs triangulating $\mathbb{H}^2$, induce a homeomorphism, or at least some appropriately behaved identification, on the boundary $\partial_\infty \mathbb{H}^2 \cong \partial\mathbb{D}$. This turns out to be true (in fact, it follows from the rigidity theorem we discuss in this remark), but non-trivial.

Proof of Theorem 4.1. The argument is by contradiction. The main idea is to superimpose the packings $\mathcal{P}$ and $\tilde{\mathcal{P}}$ on the Riemann sphere in a convenient way. In particular, we will isolate two topological quadrilaterals Q and $\tilde{Q}$ so that they are packed in combinatorially equivalent ways by disks of $\mathcal{P}$ and $\tilde{\mathcal{P}}$, but so that Q and $\tilde{Q}$ cut each other, as in Figure 6. Then the simple observation that two round disks cannot cut each other will give us our desired contradiction, via the Incompatibility Theorem 3.1.

Let $X = (V, E, F)$ be the common triangulation of $\mathbb{S}^2$ which $\mathcal{P}$ and $\tilde{\mathcal{P}}$ realize. Suppose for contradiction that $\mathcal{P}$ and $\tilde{\mathcal{P}}$ are not equivalent under any Möbius or anti-Möbius transformation. For the first part of the proof, we apply a sequence of normalizations to $\mathcal{P}$ and to $\tilde{\mathcal{P}}$. Let $f_0 = \langle v_1, v_2, v_3 \rangle \in F$ be a face of X. We first normalize via a Möbius transformation so that $D_i = \tilde{D}_i$ for $i = 1, 2, 3$. Here $D_i \in \mathcal{P}$ is the disk corresponding to the vertex $v_i \in V$ of X, similarly $\tilde{D}_i \in \tilde{\mathcal{P}}$. In particular, the correct Möbius transformation is the one that sends the intersection points of the ∂D_i to the corresponding ones of the $\partial \tilde{D}_i$.

Our next normalization is in our initial choice of f_0 and our labeling of the v_i, as per the following observation:

Observation 4.5. *Let v_4 denote the vertex of X other than v_1 so that $\langle v_2, v_3, v_4 \rangle$ is a face of X. Then there is some choice of $f_0 = \langle v_1, v_2, v_3 \rangle$ so that the disks D_4 and $\tilde{D}_4$ are not equal after our normalization identifying $D_i = \tilde{D}_i$ for $i = 1, 2, 3$.*

If there were no such choice of f_0 then in fact every pair of corresponding disks D_i and $\tilde{D}_i$ would coincide after our first normalization, and so $\mathcal{P}$ and $\tilde{\mathcal{P}}$ coincide.

An *interstice* of the packing $\mathcal{P}$ is a connected component of $\hat{\mathbb{C}} \setminus \mathcal{P}$. Every interstice is necessarily a curvilinear triangle, because the packing's contact graph triangulates $\hat{\mathbb{C}}$. For our next normalization, we insist that ∞ lies in the interstice formed by $D_1 = \tilde{D}_1, D_2 = \tilde{D}_2, D_3 = \tilde{D}_3$ which contains no other disks of either packing. Finally, we insist that $D_1 = \tilde{D}_1, D_2 = \tilde{D}_2, D_3 = \tilde{D}_3$ all have Euclidean radius 1, and that D_2 and D_3 are tangent at a point lying on the horizontal axis, so that D_1 lies to their left. The situation for $\mathcal{P}$ is depicted in Figure 9.

From now on we work in the plane $\mathbb{C}$, in the sense that $\infty \in \hat{\mathbb{C}}$ will not move again for the remainder of the proof. Note that every face f of F corresponds to some interstices $U_f \subset \mathbb{C}$ and $\tilde{U}_f \subset \mathbb{C}$ of $\mathcal{P}$ and $\tilde{\mathcal{P}}$ respectively, except for f_0, for which the interstices $U_{f_0} = \tilde{U}_{f_0}$ contain ∞. Let Q be the topological quadrilateral shown in Figure 9b. More precisely, let $V_Q = V \setminus \{v_1, v_2, v_3\}$, and let $F_Q = F \setminus \{f_0 = \langle v_1, v_2, v_3 \rangle, \langle v_2, v_3, v_4 \rangle\}$. Then we define $Q = \bigcup_{v \in V_Q} D_v \cup \bigcup_{f \in F_Q} U_f$. Define the analogous objects for $\tilde{\mathcal{P}}$ in the obvious way.

We now apply one final transformation to $\mathcal{P}$. First, suppose without loss of generality that the Euclidean radius of D_4 is larger than that of $\tilde{D}_4$. Then translate every disk of $\mathcal{P}$ to the right by a small amount $\varepsilon > 0$, leaving the disks of $\tilde{\mathcal{P}}$ unchanged. Denote this transformation by T_ε. We will discuss more precise requirements on ε later. The situation is depicted in Figure 10. The essential point is that there is an open interval of values that $\varepsilon > 0$ may take so that after all of our transformations, the topological quadrilaterals Q and $\tilde{Q}$ are arranged qualitatively as in Figure 10b. In particular, we may choose ε so that the packings of Q and $\tilde{Q}$ by the remaining disks of $\mathcal{P}$ and $\tilde{\mathcal{P}}$ are in transverse position, because there are only finitely many values of $\varepsilon > 0$ for which this fails. Then our desired contradiction follows

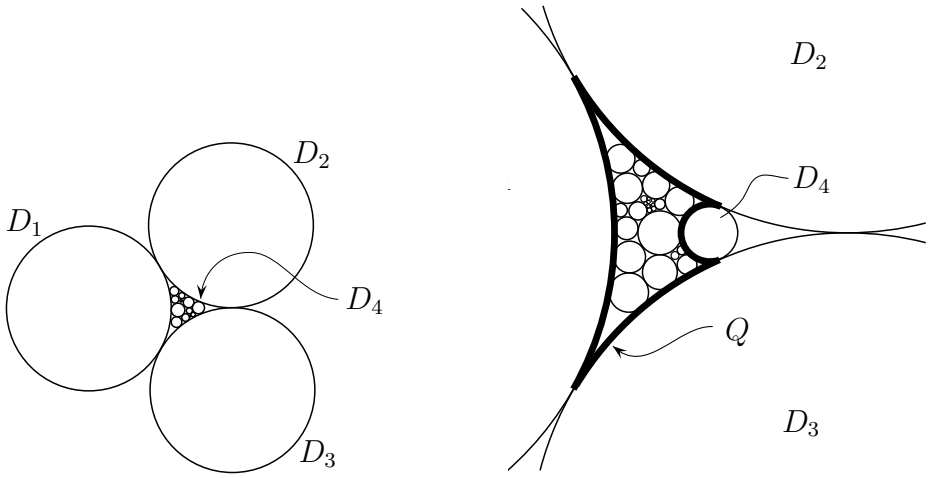

(A) (B)

FIGURE 9. **The packing $\mathcal{P}$ after some normalizations.** The disks of $\mathcal{P}$ all lie between D_1, D_2, D_3. Note that the interstice formed by D_1, D_2, D_3 on $\hat{\mathbb{C}}$ is the outside region in these figures. The disk D_4 is "the first disk of $\mathcal{P} \setminus \{D_1, D_2, D_3\}$ we get to if we start scanning from the right." In (b) the topological quadrilateral Q is outlined in bold.

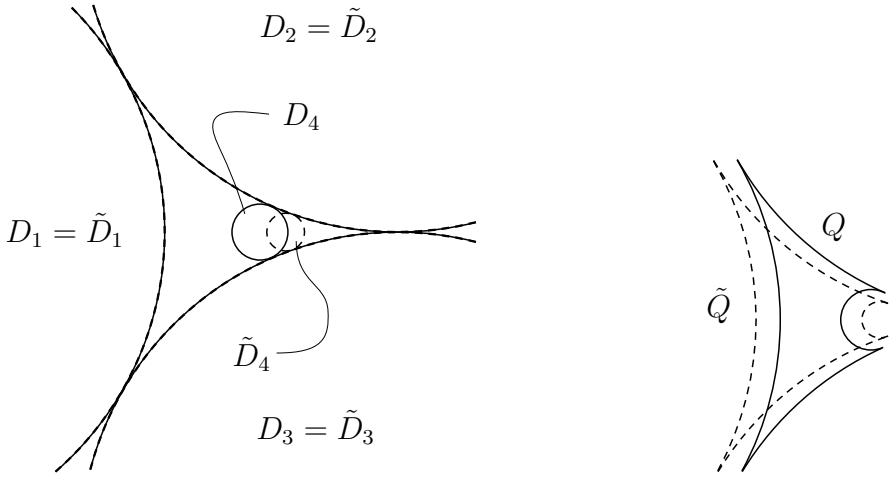

(A) (B)

FIGURE 10. **The interaction between $\mathcal{P}$ and $\tilde{\mathcal{P}}$ before and after applying T_ε.** In (a) we see the superimposition of the D_i with the $\tilde{D}_i$ before applying T_ε to $\mathcal{P}$. The disks D_i are drawn solid, and the disks $\tilde{D}_i$ are drawn dashed. In (b) we see the relative positions of Q and $\tilde{Q}$ after applying T_ε to $\mathcal{P}$.

immediately from the Incompatibility Theorem 3.1, because round closed disks cannot cut one another. □

Proof of Theorem 4.2. The proof of Theorem 4.2 proceeds along the same lines, except that after our first round of normalizations identifying D_i and $\tilde{D}_i$ for $i = 1, 2, 3$, and sending a

point of their common interstice to ∞, the remaining disks of $\mathcal{P}$ accumulate around a point $z_\infty \in \mathbb{C}$, as do those of $\tilde{\mathcal{P}}$ around a point $\tilde{z}_\infty \in \mathbb{C}$. The points z_∞ and $\tilde{z}_\infty$ may coincide or may be different. We define and apply T_ε as before, this time making sure that z_∞ and $\tilde{z}_\infty$ differ after applying T_ε.

Next, pick small disjoint neighborhoods W and $\tilde{W}$ of z_∞ and $\tilde{z}_\infty$ respectively, and contained in Q and $\tilde{Q}$ respectively. Then, let V_L be the set of vertices $v \in V$ so that both $D_v \subset W$ and $\tilde{D}_v \subset \tilde{W}$. Remove vertices from V_L until the sub-triangulation of X having vertices $V \setminus V_L$ is a triangulation of a topological closed disk. Let F_L be the set of faces of X corresponding to interstices formed by disks whose vertices are in V_L. Let L (which stands for leftovers) be the union $\bigcup_{v\in V_L} D_v \cup \bigcup_{f\in F_L} U_f \cup z_\infty$, and define $\tilde{L}$ similarly. Then $\{D_v\}_{v\in V\setminus V_L}$ together with L form a packing of the topological quadrilateral Q by closed Jordan domains, as do $\{\tilde{D}_v\}_{v\in V\setminus V_L}, \tilde{L}$ in $\tilde{Q}$. Furthermore, because L and $\tilde{L}$ are disjoint by construction, these two domains do not cut each other. Then we get our desired contradiction by the Incompatibility Theorem 3.1 as before. □

Proof of Theorem 4.3. The adaptation here is along similar lines as the adaptation to prove Theorem 4.2. Suppose for contradiction that $\mathcal{P}$ is locally finite in $\mathbb{C}$, and $\tilde{\mathcal{P}}$ is locally finite in $\mathbb{H}^2 \cong \mathbb{D}$. This time, after our normalizations, the disks of $\mathcal{P}$ accumulate around a single point z_∞, and the disks of $\tilde{\mathcal{P}}$ accumulate around some round circle C contained in the bounded region in the plane formed between $D_1 = \tilde{D}_1, D_2 = \tilde{D}_1, D_3 = \tilde{D}_3$. This time, ensure that we chose ε so that z_∞ does not lie on the circle C. We define L and $\tilde{L}$ by throwing away disks of our circle packings, as before, but this time, either L and $\tilde{L}$ are disjoint, or one contains the other. In either case, the two do not cut each other, and the conclusion of the proof proceeds as before. □

5. Torus parametrization

Before defining torus parametrization, it will be helpful to have access to the following simple lemma:

Lemma 5.1. *Suppose K and $\tilde{K}$ are closed Jordan domains in transverse position. Suppose that $z \in \partial K \cap \partial \tilde{K}$. Orient ∂K and $\partial \tilde{K}$ positively as usual. Then one of the following two mutually exclusive possibilities holds at the point z.*

(1) The curve $\partial \tilde{K}$ is entering K, and the curve ∂K is exiting $\tilde{K}$.
(2) The curve ∂K is entering $\tilde{K}$, and the curve $\partial \tilde{K}$ is exiting K.

Thus as we traverse ∂K, we alternate arriving at points of $\partial K \cap \partial \tilde{K}$ where (1) occurs and those where (2) occurs, and the same holds as we traverse $\partial \tilde{K}$.

Proof. Let $z \in \partial K \cap \partial \tilde{K}$. We may assume, by applying a homeomorphism, that locally near z the picture looks like Figure 11, with ∂K oriented down-to-up as shown. Then K lies to the left of ∂K. Now, certainly $\partial \tilde{K}$ is either entering or exiting K at z. Suppose $\partial \tilde{K}$ is entering K at z. Then $\partial \tilde{K}$ is oriented right-to-left, and so $\tilde{K}$ is below $\partial \tilde{K}$. Thus ∂K is exiting $\tilde{K}$, and case (1) occurs. Similarly, if $\partial \tilde{K}$ is exiting K at z then ∂K is entering $\tilde{K}$ at z, so case (2) occurs. □

We are now ready to define *torus parametrization*. Throughout the definition, refer to Figure 12 for an example.

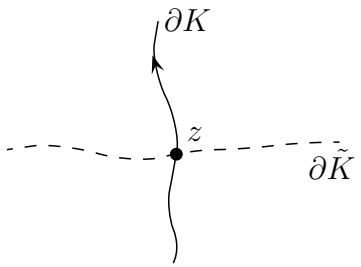

FIGURE 11. **A meeting point between two Jordan curves in transverse position.** The orientation shown on ∂K implies that K lies to the left. Depending on the orientation chosen for $\partial \tilde{K}$ we will get that $\tilde{K}$ lies above ∂K or below it.

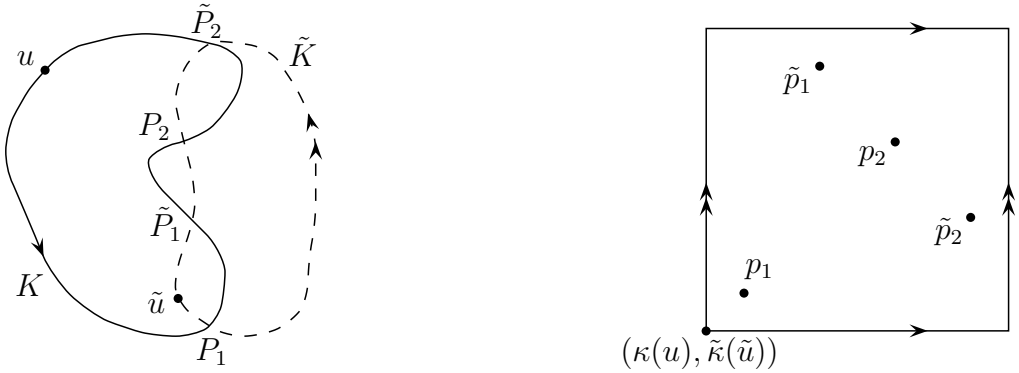

FIGURE 12. **A pair of closed Jordan domains K and $\tilde{K}$ and a torus parametrization for them, drawn with base point $(\kappa(u), \tilde{\kappa}(\tilde{u}))$.** The key points to check are that as we vary the first coordinate of $\mathbb{T}$ positively starting at u, we arrive at $\kappa(P_1)$, $\kappa(\tilde{P}_1)$, $\kappa(P_2)$, and $\kappa(\tilde{P}_2)$ in that order, and as we vary the second coordinate of $\mathbb{T}$ positively starting at $\tilde{\kappa}(\tilde{u})$, we arrive at $\tilde{\kappa}(P_1)$, $\tilde{\kappa}(\tilde{P}_2)$, $\tilde{\kappa}(P_2)$, and $\tilde{\kappa}(P_1)$ in that order.

Definition 5.2. Let K and $\tilde{K}$ be closed Jordan domains in transverse position, so that ∂K and $\partial \tilde{K}$ meet at $2M \geq 0$ points, with boundaries oriented as usual. Let $\partial K \cap \partial \tilde{K} = \{P_1, \ldots, P_M, \tilde{P}_1, \ldots, \tilde{P}_M\}$, where P_i and $\tilde{P}_i$ are labeled so that at every P_i we have that ∂K is entering $\tilde{K}$, and at every $\tilde{P}_i$ we have that $\partial \tilde{K}$ is entering K. Imbue $\mathbb{S}^1$ with an orientation and let $\kappa : \partial K \to \mathbb{S}^1$ and $\tilde{\kappa} : \partial \tilde{K} \to \mathbb{S}^1$ be orientation-preserving homeomorphisms. We refer to this as fixing a *torus parametrization* for K and $\tilde{K}$.

We consider a point (x, y) on the 2-torus $\mathbb{T} = \mathbb{S}^1 \times \mathbb{S}^1$ to be parametrizing simultaneously a point $\kappa^{-1}(x) \in \partial K$ and a point $\tilde{\kappa}^{-1}(y) \in \partial \tilde{K}$. We denote by $p_i \in \mathbb{T}$ be the unique point $(x, y) \in \mathbb{T}$ satisfying $\kappa^{-1}(x) = \tilde{\kappa}^{-1}(y) = P_i$, similarly $\tilde{p}_i \in \mathbb{T}$. Note that by the transverse position hypothesis no pair of points in $\{p_1, \ldots, p_M, \tilde{p}_1, \ldots, \tilde{p}_M\}$ share a first coordinate, nor a second coordinate.

Suppose we pick $(x_0, y_0) \in \mathbb{S}^1 \times \mathbb{S}^1$. Then we may draw an image of $\mathbb{T} = \mathbb{S}^1 \times \mathbb{S}^1$ by letting $\{x_0\} \times \mathbb{S}^1$ be the vertical axis and letting $\mathbb{S}^1 \times \{y_0\}$ be the horizontal axis. Then we call (x_0, y_0) a *base point* for the drawing.

Suppose that $\phi : \partial K \to \partial \tilde{K}$ is an orientation-preserving homeomorphism. Then ϕ determines an oriented curve γ in $\mathbb{T}$ for us, namely its graph $\gamma = \{(\kappa(z), \tilde{\kappa}(\phi(z))\}_{z \in \partial K}$, with

orientation obtained by traversing ∂K positively. Note that ϕ is fixed-point-free if and only if its associated curve γ misses all of the p_i and $\tilde{p}_i$. Pick $u \in \partial K$ and denote $\tilde{u} = \phi(u)$. Then if we draw the torus parametrization for K and $\tilde{K}$ using the base point $(\kappa(u), \tilde{\kappa}(\tilde{u}))$, the curve γ associated to ϕ "looks like the graph of a strictly increasing function." The converse is also true: given any such γ, it determines for us an orientation-preserving homeomorphism $\partial K \to \partial \tilde{K}$ sending u to $\tilde{u}$, which is fixed-point-free if and only if γ misses all of the p_i and $\tilde{p}_i$.

Suppose that $\phi(u) = \tilde{u}$, equivalently that $(\kappa(u), \tilde{\kappa}(\tilde{u})) \in \gamma$. The curve γ and the horizontal and vertical axes $\{\tilde{\kappa}(\tilde{u})\} \times \mathbb{S}^1$ and $\mathbb{S}^1 \times \{\kappa(u)\}$ divide $\mathbb{T}$ into two simply connected open sets $\Delta_\uparrow(u, \gamma)$ and $\Delta_\downarrow(u, \gamma)$ as shown in Figure 13. We suppress the dependence on $\tilde{u}$ in the notation because $\tilde{u} = \phi(u)$. If neither $u \in \partial \tilde{K}$ nor $\tilde{u} \in \partial K$ then every p_i and every $\tilde{p}_i$ lies in either $\Delta_\downarrow(u, \gamma)$ or $\Delta_\uparrow(u, \gamma)$. In this case we write $\#p_\downarrow(u, \gamma)$ to denote $|\{p_1, \ldots, p_M\} \cap \Delta_\downarrow(u, \gamma)|$ the number of points p_i which lie in $\Delta_\downarrow(u, \gamma)$, and we define $\#p_\uparrow(u, \gamma)$, $\#\tilde{p}_\downarrow(u, \gamma)$, and $\#\tilde{p}_\uparrow(u, \gamma)$ in the analogous way. Denote by $\omega(\alpha, z)$ the winding number of the closed curve $\alpha \subset \mathbb{C}$ around the point $z \notin \alpha$.

The following central lemma says that given an indexable homeomorphism $\phi : \partial K \to \partial \tilde{K}$, we may read off its fixed-point index $\eta(\phi)$ simply by examining the curve γ associated to ϕ in the way we just described:

Lemma 5.3. *Let K and $\tilde{K}$ be closed Jordan domains. Fix a torus parametrization of K and $\tilde{K}$ via κ and $\tilde{\kappa}$. Let $\phi : \partial K \to \partial \tilde{K}$ be an indexable homeomorphism, with graph γ in $\mathbb{T}$. Suppose that $\phi(u) = \tilde{u}$, where $u \notin \partial \tilde{K}$ and $\tilde{u} \notin \partial K$. Then:*

$$\eta(\phi) = w(\gamma) = \omega(\partial K, \tilde{u}) + \omega(\partial \tilde{K}, u) - \#p_\downarrow(u, \gamma) + \#\tilde{p}_\downarrow(u, \gamma) \tag{1}$$

$$= \omega(\partial K, \tilde{u}) + \omega(\partial \tilde{K}, u) + \#p_\uparrow(u, \gamma) - \#\tilde{p}_\uparrow(u, \gamma) \tag{2}$$

The remainder of the section is spent proving Lemma 5.3.

Suppose γ_0 is any oriented closed curve in $\mathbb{T} \setminus \{p_1, \ldots, p_M, \tilde{p}_1, \ldots, \tilde{p}_M\}$. Then the closed curve $\{\tilde{\kappa}^{-1}(y) - \kappa^{-1}(x)\}_{(x,y) \in \gamma_0}$ misses the origin, and has a natural orientation obtained by traversing γ_0 positively. We denote by $w(\gamma_0)$ the winding number around the origin of $\{\tilde{\kappa}^{-1}(y) - \kappa^{-1}(x)\}_{(x,y) \in \gamma_0}$.

Observation 5.4. *If γ_1 and γ_2 are homotopic in $\mathbb{T} \setminus \{p_1, \ldots, p_M, \tilde{p}_1, \ldots, \tilde{p}_M\}$ then $w(\gamma_1) = w(\gamma_2)$.*

This is because the homotopy between γ_1 and γ_2 in $\mathbb{T} \setminus \{p_2, \ldots, p_M, \tilde{p}_1, \ldots, \tilde{p}_M\}$ induces a homotopy between the closed curves $\{\tilde{\kappa}^{-1}(y) - \kappa^{-1}(x)\}_{(x,y) \in \gamma_1}$ and $\{\tilde{\kappa}^{-1}(y) - \kappa^{-1}(x)\}_{(x,y) \in \gamma_2}$ in the punctured plane $\mathbb{C} \setminus \{0\}$.

Suppose that $\phi : \partial K \to \partial \tilde{K}$ is a fixed-point-free orientation-preserving homeomorphism. Let γ be its graph in $\mathbb{T}$. If γ has orientation induced by traversing ∂K and $\partial \tilde{K}$ positively, then the following is a tautology.

Observation 5.5. $\eta(\phi) = w(\gamma)$

Orient $\partial \Delta_\downarrow(u, \gamma)$ as shown in Figure 13. Then $\partial \Delta_\downarrow(u, \gamma)$ is the concatenation of the curve γ traversed backwards with $\mathbb{S}^1 \times \{\tilde{\kappa}(\tilde{u})\}$ and $\{\kappa(u)\} \times \mathbb{S}^1$, where the two latter curves are oriented according to the positive orientation on $\mathbb{S}^1$.

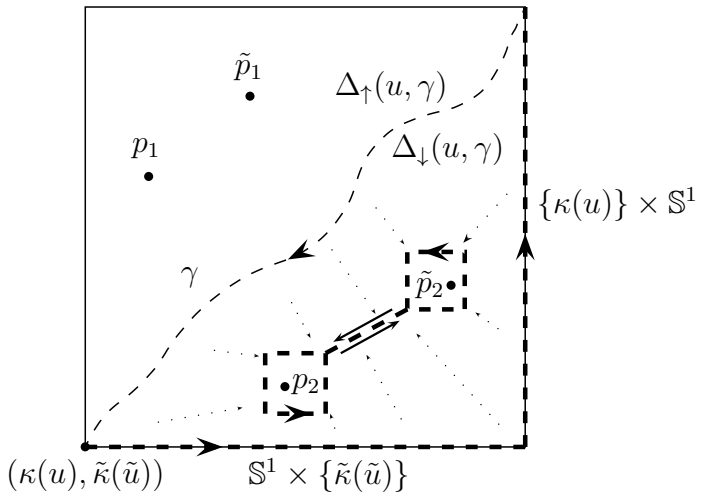

FIGURE 13. **A homotopy from $\partial\Delta_\downarrow(u,\gamma)$ to Γ.** Here the orientation shown on γ is the opposite of the orientation induced by traversing ∂K positively.

Observation 5.6. *If $\mathbb{S}^1\times\{\tilde{\kappa}(\tilde{u})\}$ and $\{\kappa(u)\}\times\mathbb{S}^1$ are oriented according to the positive orientation on $\mathbb{S}^1$, then $w(\mathbb{S}^1\times\{\tilde{\kappa}(\tilde{u})\})=\omega(\partial K,\tilde{u})$ and $w(\{\kappa(u)\}\times\mathbb{S}^1)=\omega(\partial\tilde{K},u)$.*

It is also easy to see that if we concatenate two closed curves γ_1 and γ_2 that meet at a point, we get $w(\gamma_1\circ\gamma_2)=w(\gamma_1)+w(\gamma_2)$. Thus in light of the orientations on $\partial\Delta_\downarrow(u,\gamma)$ and all other curves concerned we get:

$$\begin{aligned} w(\partial\Delta_\downarrow(u,\gamma)) &= w(\mathbb{S}^1\times\{\tilde{\kappa}(\tilde{u})\})+w(\{\kappa(u)\}\times\mathbb{S}^1)-w(\gamma)\\ &= \omega(\partial K,\tilde{u})+\omega(\partial\tilde{K},u)-\eta(\phi)\end{aligned}$$

For every i let $\zeta(p_i)$ and $\zeta(\tilde{p}_i)$ be small squares around p_i and $\tilde{p}_i$ respectively in $\mathbb{T}$, oriented as shown in Figure 13. By *square* we mean a simple closed curve which decomposes into four "sides," so that on a given side one of the two coordinates of $\mathbb{S}^1\times\mathbb{S}^1=\mathbb{T}$ is constant. Pick the rectangles small enough so that the closed boxes they bound are pairwise disjoint and do not meet $\partial\Delta_\downarrow(u,\gamma)$.

Let Γ be the closed curve in $\Delta_\downarrow(u,\gamma)$ obtained in the following way. First, start with every loop $\zeta(p_i)$ and $\zeta(\tilde{p}_i)$ for those p_i and $\tilde{p}_i$ lying in $\Delta_\downarrow(u,\gamma)$. Let δ_0 be an arc contained in the interior of $\Delta_\downarrow(u,\gamma)$ which meets each $\zeta(p_i)$ and $\zeta(\tilde{p}_i)$ contained in $\Delta_\downarrow(u,\gamma)$ at exactly one point. It is easy to prove inductively that such an arc exists. Let δ be the closed curve obtained by traversing δ_0 first in one direction, then in the other. Then let Γ be obtained by concatenating δ with every $\zeta(p_i)$ and $\zeta(\tilde{p}_i)$ contained in $\Delta_\downarrow(u,\gamma)$.

Observation 5.7. *The curves Γ and $\partial\Delta_\downarrow(u,\gamma)$ are homotopic in $\mathbb{T}\setminus\{p_1,\dots,p_M,\tilde{p}_1,\dots,\tilde{p}_M\}$. Also $w(\delta)=0$. It follows that:*

$$w(\partial\Delta_\downarrow(u,\gamma))=w(\Gamma)=\sum_{p_i\in\Delta_\downarrow(u,\gamma)}w(\zeta(p_i))+\sum_{\tilde{p}_i\in\Delta_\downarrow(u,\gamma)}w(\zeta(\tilde{p}_i))$$

See Figure 13 for an example. On the other hand, the following holds.

Observation 5.8. *$w(\zeta(p_i))=1$, $w(\zeta(\tilde{p}_i))=-1$*

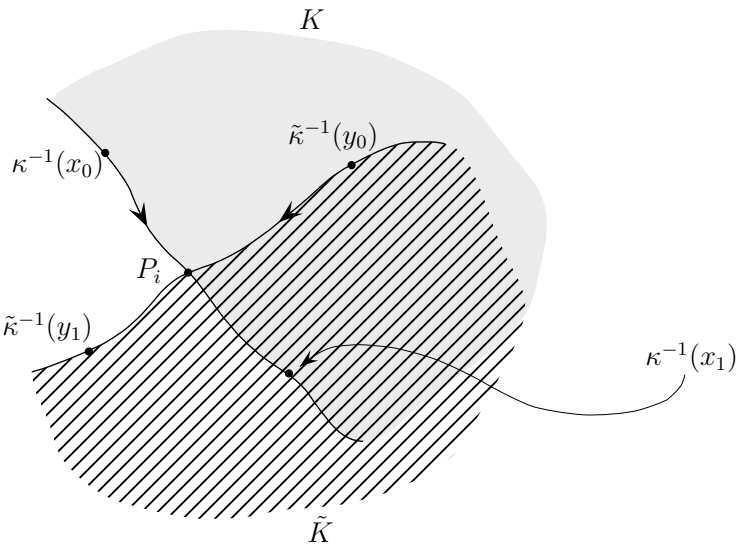

FIGURE 14. **The local picture near P_i.** This allows us to compute the "local fixed-point index" $w(\zeta(p_i))$ of f near P_i.

To see why, suppose that $\zeta(p_i) = \partial([x_0 \to x_1]_{\mathbb{S}^1} \times [y_0 \to y_1]_{\mathbb{S}^1})$. Then up to orientation-preserving homeomorphism the picture near P_i is as in Figure 14. We let (x, y) traverse $\zeta(p_i)$ positively starting at (x_0, y_0), keeping track of the vector $\tilde{\kappa}^{-1}(y) - \tilde{\kappa}^{-1}(x)$ as we do so. The vector $\tilde{\kappa}^{-1}(y_0) - \tilde{\kappa}^{-1}(x_0)$ points to the right. As x varies from x_0 to x_1, the vector $\tilde{\kappa}^{-1}(y) - \tilde{\kappa}^{-1}(x)$ rotates in the positive direction, that is, counter-clockwise, until it arrives at $\tilde{\kappa}^{-1}(y_0) - \kappa^{-1}(x_1)$, which points upward. Continuing in this fashion, we see that $\tilde{\kappa}^{-1}(y) - \tilde{\kappa}^{-1}(x)$ makes one full counter-clockwise rotation as we traverse $\zeta(p_i)$. The proof that $w(\zeta(\tilde{p}_i)) = -1$ is similar. Combining all of our observations establishes equation 1. The proof that equation 2 holds is similar. □

6. Proof of the Three Point Prescription Lemma 1.2

We restate the lemma for the convenience of the reader. Let K and $\tilde{K}$ be compact Jordan domains in transverse position. Let $z_1, z_2, z_3 \in \partial K \setminus \partial \tilde{K}$ appear in counterclockwise order, similarly $\tilde{z}_1, \tilde{z}_2, \tilde{z}_3 \in \partial \tilde{K} \setminus \partial K$. An indexable homeomorphism $\phi : \partial K \to \partial \tilde{K}$ is called *faithful* if it sends $z_i \mapsto \tilde{z}_i$ for $i = 1, 2, 3$. We wish to find a faithful ϕ with $\eta(\phi) \geq 0$. We refer to the z_i and the $\tilde{z}_i$ as our *constraint points*.

We proceed by induction on the number of intersection points $\partial K \cap \partial \tilde{K}$, noting that this number is always even. The Circle Index Lemma 2.1 takes care of the cases where ∂K and $\partial \tilde{K}$ meet 0 or 2 times. Thus suppose that ∂K and $\partial \tilde{K}$ meet at least 4 times.

The main idea of the proof is to find sub-arcs of ∂K and $\partial \tilde{K}$ which "cross minimally," and "pull them apart," see Figure 15. When "pulling these sub-arcs apart," we leave the rest of ∂K and $\partial \tilde{K}$ fixed, as in Figure 16. We then apply the induction hypothesis to the resulting Jordan domains K' and $\tilde{K}'$, obtaining some indexable homeomorphism $\phi' : \partial K' \to \partial \tilde{K}'$ with $\eta(\phi') \geq 0$. Finally, we use ϕ' to construct ϕ, arguing that the fixed-point index is preserved or increased in this last step. The details of the proof will be worked out in a torus parametrization. This is because the torus parametrization allows us to work systematically and somewhat combinatorially through many cases, and unfortunately much of the proof is

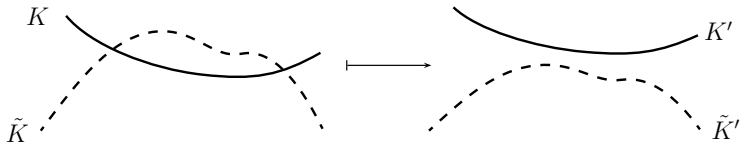

FIGURE 15. **"Pulling apart" two sub-curves of ∂K and $\partial\tilde{K}$ "crossing minimally."** Note that *a priori* the orientations on ∂K and $\partial\tilde{K}$ may be arbitrary, so the open Jordan domain formed between the two curves on the left may be contained in both K and $\tilde{K}$, in just one of them, or in neither.

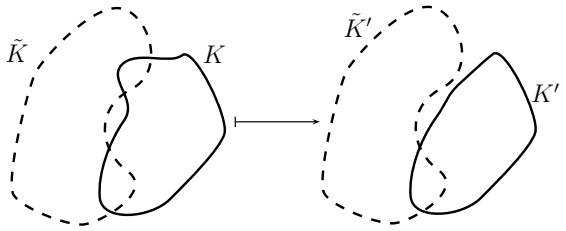

FIGURE 16. **The compact Jordan domains under consideration, before and after "pulling the sub-arcs apart."** Note that in this case, we had three choices of which arcs to pull apart, and each choice results in a different pair $K', \tilde{K}'$.

case analysis. Also unfortunately, it is often difficult to discuss the plane topological pictures under consideration using prose, so much of the proof involves chasing the definitions of various terms and mathematical expressions around.

6.1. **Initial set-up.** Two intersection points $p_0, \tilde{p}_0 \in \partial K \cap \partial\tilde{K}$ are called *adjacent in* ∂K if one of the two arcs $[p_0 \to \tilde{p}_0]_{\partial K}$ and $[\tilde{p}_0 \to p_0]_{\partial K}$ does not contain any other intersection points $\partial K \cap \partial\tilde{K}$. Note that two intersection points of $\partial K \cap \partial\tilde{K}$ may be adjacent only if ∂K enters $\tilde{K}$ at one and leaves $\tilde{K}$ at the other, so our notation is in keeping with our conventions from Section 5. We define *adjacency in* $\partial\tilde{K}$ similarly.

Two intersection points $p_0, \tilde{p}_0 \in \partial K \cap \partial\tilde{K}$ are called *doubly adjacent* if they are adjacent both in ∂K and in $\partial\tilde{K}$. Then the notion of sub-arcs of ∂K and $\partial\tilde{K}$ "crossing minimally" which we informally described before is exactly captured by the property of double adjacency. If $\partial K \cap \partial\tilde{K}$ meet, then there is always at least one doubly adjacent pair of points in $\partial K \cap \partial\tilde{K}$.

From now on, we fix a torus parametrization of ∂K and $\partial\tilde{K}$ in $\mathbb{T} = \mathbb{S}^1 \times \mathbb{S}^1$ via $\kappa : \partial K \to \mathbb{S}^1$ and $\tilde{\kappa} : \partial\tilde{K} \to \mathbb{S}^1$. Let $p_0, \tilde{p}_0$ be doubly adjacent. Then we denote $P_0 = (\kappa(p_0), \tilde{\kappa}(p_0))$ and $\tilde{P}_0 = (\kappa(\tilde{p}_0), \tilde{\kappa}(\tilde{p}_0))$ as usual, so $P_0 \in \mathbb{T}$ parametrizes the point $p_0 \in \partial K \cap \partial\tilde{K}$, similarly $\tilde{P}_0$ for $\tilde{p}_0$. We can now see how we plan to apply induction:

Observation 6.1. *Let the torus parametrization $\mathbb{T}'$ be obtained from $\mathbb{T}$ by deleting P_0 and $\tilde{P}_0$. Then $\mathbb{T}'$ parametrizes a pair $\partial K'$ and $\partial\tilde{K}'$, where K' and $\tilde{K}'$ are compact Jordan domains in transverse position, meeting two times fewer than do K and $\tilde{K}$.*

Thus our strategy will be as follows: first, apply the induction hypothesis to $\mathbb{T}'$, to get a faithful indexable γ' so that $w(\gamma') = \eta(\phi') \geq 0$; then, "reinsert" the points P_0 and $\tilde{P}_0$, in such a way that the fixed-point index is preserved or increased.

6.2. **Partitioning $\mathbb{T}$.** We will refer to the collection of the sets $\mathbb{S}^1 \times \{\tilde{\kappa}(\tilde{z}_i)\}$ and $\{\kappa(z_i)\} \times \mathbb{S}^1$ for $i = 1, 2, 3$ as our *grid lines*, and to their pairwise intersection points as our *lattice points*.

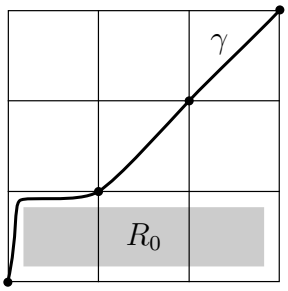

FIGURE 17. **The situation if all P_i and $\tilde{P}_i$ lie in a single lattice row.** Here we have supposed that they lie in the bottom lattice row, in which case they in fact lie in some open rectangle R_0 contained in the bottom lattice row.

Furthermore we refer to the points $(\kappa(z_i), \tilde{\kappa}(\tilde{z}_i))$, for $i = 1, 2, 3$, as our *constraint lattice points*. If we draw our torus parametrization with a lattice point chosen to be the base point, then the grid lines actually divide the drawing into a grid, with nine disjoint rectangular cells in total. We will refer to these as our *lattice cells*. Within any lattice cell there are well-defined left, right, up, and down directions.

From now on, whenever we draw the torus parametrization $\mathbb{T}$, we will always pick one of the lattice points for the base point. Suppose for the rest of this paragraph that we have fixed such a drawing. Then we may refer to the lattice cells according to their position in this drawing in the natural way, for example we may refer to the bottom-left lattice cell. We denote the lattice cells by $C_\uparrow, C_\nearrow, C_\rightarrow, \ldots, C_\leftarrow, C_\nwarrow$ in the natural way, and write $C_\bullet$ to denote the central lattice cell. Then the union of the closed upper-left, middle-left, and lower-left lattice cells is called the *left lattice column*. We define the *central* and *right lattice columns* analogously, as well as the *bottom*, *central*, and *top lattice rows*. We again emphasize that these descriptors depend crucially on the choice of base point for the drawing of the torus parametrization.

As usual, we denote $P_i = (\kappa(p_i), \tilde{\kappa}(p_i))$ and $\tilde{P}_i = (\kappa(\tilde{p}_i), \tilde{\kappa}(\tilde{p}_i))$, where $\{p_i, \tilde{p}_i\} = \partial K \cap \partial \tilde{K}$, with the same notational conventions as in Section 5. We will apply Lemma 5.3 frequently. Before moving on to the next part of the proof, we make an observation that will simplify things later:

Observation 6.2. *Suppose that all of the P_i and $\tilde{P}_i$ lie in a single lattice row, or in a single lattice column. Then Lemma 1.2 holds, without the need for induction.*

To see why, we walk through Figure 17. We suppose that all of the P_i and $\tilde{P}_i$ lie in a single lattice row, call it R. The same argument will work if they all lie in a single lattice column. Without loss of generality, we have drawn the torus parametrization so that R is the bottom lattice row, and so that the base point is a constraint lattice point. We may do so by picking the correct constraint lattice point to serve as our base point. Then the other two constraint lattice points are the ones along the diagonal, drawn in the figure as dots. As usual, a faithful indexable homeomorphism $\phi : \partial K \to \partial \tilde{K}$ can be parametrized by a "strictly increasing" curve

- from the bottom-left corner of the bottom-left cell,
- to the top-right corner of the top-right cell,
- passing through the two other constraint lattice points, and

- missing all of the P_i and $\tilde{P}_i$.

Thus the γ we have drawn in Figure 17 parametrizes such a homeomorphism. Furthermore, because there are finitely many P_i and $\tilde{P}_i$, and all of them lie in the bottom lattice row R, in fact they lie in an open rectangle R_0 as depicted in Figure 17. Thus $\eta(\phi) \geq 0$ by Lemma 5.3.

6.3. **The adjacency box.** Let p_0 and $\tilde{p}_0$ be adjacent in ∂K, and let a_0 denote the arc connecting p_0 and $\tilde{p}_0$ along ∂K which contains no other intersection points $\partial K \cap \partial \tilde{K}$. Thus a_0 is equal to one of $[p_0 \to \tilde{p}_0]_{\partial K}$ and $[\tilde{p}_0 \to p_0]_{\partial K}$. There is a unique such a_0 so long as ∂K and $\partial \tilde{K}$ meet at least four times, as is our running assumption. We call this a_0 the *short adjacency arc of* $p_0, \tilde{p}_0$ *in* ∂K, and define the *short adjacency arc* $\tilde{a}_0$ *of* $p_0, \tilde{p}_0$ *in* $\partial \tilde{K}$ similarly.

Continuing with the notation of the last paragraph, let a be obtained from a_0 by extending it slightly on both ends, so that $a \subset \partial K$ is a closed Jordan arc containing p_0 and $\tilde{p}_0$, but no other points of $\partial K \cap \partial \tilde{K}$, and no constraint point z_i which was not already contained in a_0. There is a topologically unique such a. Then we say that a is the *adjacency arc of* $p_0, \tilde{p}_0$ *in* ∂K of $p_0, \tilde{p}_0$. We define the *adjacency arc* $\tilde{a}$ *of* $p_0, \tilde{p}_0$ *in* $\partial \tilde{K}$ similarly.

Again continuing with the notation of before, let $A = \kappa(a) \times \tilde{\kappa}(\tilde{a}) \subset \mathbb{T} = \mathbb{S}^1 \times \mathbb{S}^1$ be the closed rectangle so that $(x, \tilde{x}) \in A$ if and only if $\kappa^{-1}(x) \in a$ and $\tilde{\kappa}^{-1}(\tilde{x}) \in \tilde{a}$. Because a and $\tilde{a}$ are essentially unique, we get also that there is a topologically unique such A. Then A is called the *adjacency box* of $p_0, \tilde{p}_0$.

6.4. **Enumerating the possible locations of the adjacency box.** Pick doubly adjacent $p_0, \tilde{p}_0$, having adjacency arcs $a_0, \tilde{a}_0$ and let $A = \kappa(a_0) \times \tilde{\kappa}(\tilde{a}_0) \subset \mathbb{T}$ be their adjacency box. Let $b_0 = \partial K \setminus a_0$ and $\tilde{b}_0 = \partial \tilde{K} \setminus b_0$, and set $B = \kappa(b_0) \times \tilde{\kappa}(\tilde{b}_0) \subset \mathbb{T}$. Then the parametrization in $\mathbb{T}$ of every point in $\partial K \cap \partial \tilde{K} \setminus \{p_0, \tilde{p}_0\}$ lies B. However, we have basically no *a priori* information about how these points are arranged in B. However:

Observation 6.3. *Suppose that $z_1, z_2, z_3 \in a_0$. Then $b_0 \times \mathbb{S}^1 \supset B$ is contained in a lattice column, regardless of which lattice point is chosen for the base point of our drawing of the torus parametrization. Thus Lemma 1.2 holds by Observation 6.2.*

Thus we may assume without loss of generality that some z_i does not lie in a. Similarly, one of the $\tilde{z}_i$ lies outside of $\tilde{a}$. This allows us to conclude the following:

Observation 6.4. *We may suppose without loss of generality that A meets the left lattice column.*

To see why, let $z_i \in z_1, z_2, z_3$ be so that $z_i \notin a_0$. Then traverse ∂K starting from z_i, positively, until arriving at the initial endpoint of a_0. Let z_j be the last one of z_1, z_2, z_3 crossed during this traversal. Then we may draw the torus parametrization using $(\kappa(z_j), \tilde{\kappa}(\tilde{z}_j))$ as the base point.

After relabeling if necessary, we suppose from now on that our torus parametrization is drawn with $(\kappa(z_1), \tilde{\kappa}(\tilde{z}_1))$ as our base point. In particular, this means that $z_1 \notin a$, so our adjacency box A does not meet the left, nor the right grid line $\{\kappa(z_1)\} \times \mathbb{S}^1$ of our torus parametrization.

Because A is a topological rectangle in the natural way, it has well-defined left, right, up, and down directions. More precisely, we suppose that the positive orientation on the first coordinate of $\mathbb{T} = \mathbb{S}^1 \times \mathbb{S}^1$ goes left-to-right, and on the second coordinate goes down-to-up. Then:

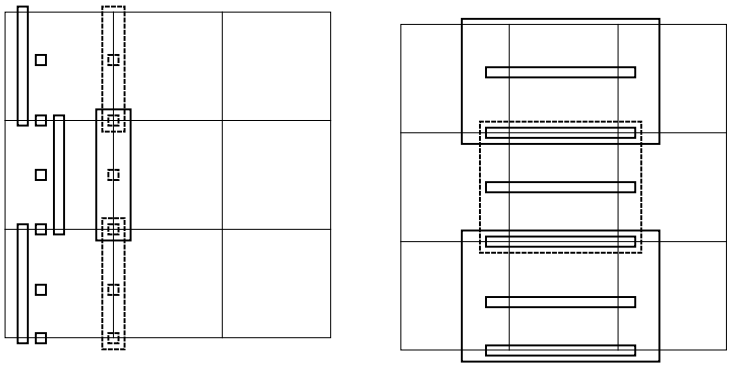

(A) (B)

FIGURE 18. **The 27 possible topologically distinct locations for the adjacency box A.** Both torus parametrizations are drawn with $(\kappa(z_1), \tilde{\kappa}(\tilde{z}_1))$ as the base point. In (a) we have cases (r, s) where $t \neq \nearrow, \rightarrow, \searrow$. The adjacency box A is shown with a solid boundary for the cases $s = \nwarrow, \leftarrow, \swarrow$, and with a dashed boundary for the cases $r = \uparrow, \bullet, \downarrow$, except for the case $(\swarrow, \uparrow)$, which is shown with a solid boundary. In (b), we have cases (r, s) where $s = \nearrow, \rightarrow, \searrow$. Here the adjacency box A is drawn with a solid boundary, except for the case $(\swarrow, \nearrow)$, which is shown with a dashed boundary. When a sample location for the adjacency box is drawn hanging off of the bottom of $\mathbb{T}$, or over the top, we think of it as "wrapping around" to the cell vertically opposite, in accordance with the identification of the top and bottom grid lines of $\mathbb{T}$.

Observation 6.5. *Under our running assumptions, the topological location of A in the torus parametrization is completely determined by two pieces of information:*

- *which of the cells of the left lattice column contains the lower-left corner $A_{\swarrow}$ of A, and*
- *which of the nine lattice cells contains the upper-right corner $A_{\nearrow}$ of A.*

We will denote the cases for the topological location of A in the following way: let r equal one of $\swarrow, \leftarrow, \nwarrow$, and let s equal one of $\uparrow, \nearrow, \rightarrow, \ldots, \leftarrow, \nwarrow, \bullet$. Then we say that case (r, s) occurs if and only if $A_{\swarrow}$ lies in lattice cell C_r, and $A_{\nearrow}$ lies in lattice cell C_s. *A priori* this gives us $3 \times 9 = 27$ possibilities for A. Fortunately we will see that many of the cases are handled in more or less the same way. For reference we have depicted the 27 cases in Figure 18.

6.5. **First application of induction, when γ misses A.** For the remainder of the proof, let $\mathbb{T}'$ be the torus parametrization obtained from $\mathbb{T}$ by simply deleting P_0 and $\tilde{P}_0$, and let γ' be the curve in $\mathbb{T}'$ obtained inductively as described in Observation 6.1, so that in particular $w(\gamma') \geq 0$. We wish to construct γ in $\mathbb{T}$ from γ', so that $w(\gamma) \geq w(\gamma') \geq 0$. In comparing $w(\gamma)$ with $w(\gamma')$, the germane issue is the effect of the presence of $P_0, \tilde{P}_0$ in $\mathbb{T}$ compared to their absence from $\mathbb{T}'$. In light of Lemma 5.3, there are precisely two ways that reinserting these points can change the fixed-point indices under consideration:

- First, they may affect the winding numbers $\omega(\partial K', \tilde{z}_1')$ and $\omega(\partial \tilde{K}', z_1')$ as compared to $\omega(\partial K, \tilde{z}_1)$ and $\omega(\partial \tilde{K}, z_1)$. Here $K', \tilde{K}'$ are the closed Jordan domains parametrized by the torus parametrization $\mathbb{T}'$.

- Second, they may affect the sum $-\#p_\downarrow(z_1,\gamma) + \#\tilde{p}_\downarrow(z_1,\gamma)$, equivalently the sum $\#p_\uparrow(z_1,\gamma) - \#\tilde{p}_\uparrow(z_1,\gamma)$, as compared to the respective sums in $\mathbb{T}'$.

We have the following nice observation:

Observation 6.6. *The winding numbers $\omega(\partial K, \tilde{z}_1)$ and $\omega(\partial K', \tilde{z}_1')$ are equal.*

This is because $\omega(\partial K, \tilde{z}_1)$ is determined completely by whether we arrive first at a $\kappa(p_i)$ or a $\kappa(\tilde{p}_i)$ as we traverse the first coordinate $\mathbb{S}^1$ of $\mathbb{T}$ positively starting at $\kappa(z_1)$, and this is invariant under reinserting $P_0, \tilde{P}_0$, as the points p_0 and $\tilde{p}_0$ occur immediately after one another, in some order, as we traverse ∂K starting at z_1.

The following claim will prove useful:

Next:

Claim 6.7. *Suppose that $\gamma = \gamma'$ does not meet A. Then $w(\gamma) = w(\gamma') \geq 0$.*

Proof. There are two cases, handled differently:

Case 1. The box A does not meet the bottom/top grid line $\mathbb{S}^1 \times \{\tilde{\kappa}(\tilde{z}_1)\}$.

In this case, similarly to Observation 6.6, we get that $\omega(\partial\tilde{K}, z_1) = \omega(\partial\tilde{K}', z_1')$. Also, because $\gamma = \gamma'$ does not meet A, we have that P_0 and $\tilde{P}_0$ either both lie above γ in $\mathbb{T}$, or both lie below it. Thus $-\#p_\downarrow(z_1,\gamma) + \#\tilde{p}_\downarrow(z_1,\gamma) = -\#p_\downarrow(z_1,\gamma') + \#\tilde{p}_\downarrow(z_1,\gamma')$, completing the proof of the claim by Lemma 5.3.

Case 2. The box A crosses the bottom/top grid line $\mathbb{S}^1 \times \{\tilde{\kappa}(\tilde{z}_1)\}$.

In this case, the bottom/top grid line $\mathbb{S}^1 \times \{\tilde{\kappa}(\tilde{z}_1)\}$ cuts A into two connected components $A_\downarrow$ and $A_\uparrow$, one of which contains P_0 and the other of which contains $\tilde{P}_0$. The "upper half" of A, which we have denoted $A_\uparrow$, actually lies in the bottom lattice row of $\mathbb{T}$, and furthermore lies beneath γ because γ does not meet A. Similarly $A_\downarrow$ lies in the upper lattice row of $\mathbb{T}$ and above γ. There are two sub-cases:

Sub-case 2.1. $P_0 \in A_\downarrow$, $\tilde{P}_0 \in A_\uparrow$

In this case $-\#p_\downarrow(z_1,\gamma) + \#\tilde{p}_\downarrow(z_1,\gamma)$ in $\mathbb{T}$ is 1 less than $-\#p_\downarrow(z_1,\gamma') + \#\tilde{p}_\downarrow(z_1,\gamma')$ in $\mathbb{T}'$. On the other hand $\omega(\partial\tilde{K}, z_1) = 1$ and $\omega(\partial\tilde{K}', z_1') = 0$. Thus the total change between indices in the two settings cancels out and we get $w(\gamma) = w(\gamma')$ by Lemma 5.3.

Sub-case 2.2. $P_0 \in A_\uparrow$, $\tilde{P}_0 \in A_\downarrow$

This sub-case is handled in the same way as Sub-case 2.1, except that this time $\omega(\partial\tilde{K}, z_1) + 1 = \omega(\partial\tilde{K}', z_1')$ and $-\#p_\downarrow(z_1,\gamma) = -\#p_\downarrow(z_1,\gamma') + 1$. This completes the proof of Claim 6.7. □

Much of the rest of the proof of Lemma 1.2 will be spent trying to reduce to the situation handled by Claim 6.7.

6.6. **Moving $P_0, \tilde{P}_0$, or adjusting A.** We continue with the notation from before. *A priori* there are exactly four topologically distinct ways that P_0 and $\tilde{P}_0$ may be arranged in the adjacency box A of $p_0, \tilde{p}_0$, as depicted in Figure 19.

The following observation will be helpful later:

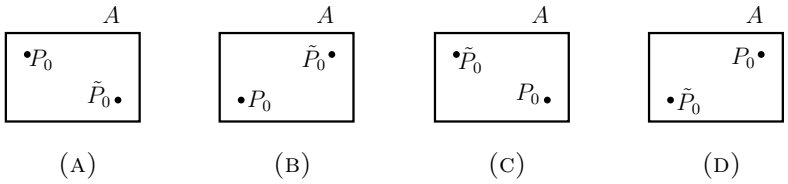

FIGURE 19. **The *a priori* possible arrangements of $P_0, \tilde{P}_0$ in the adjacency box B.**

Observation 6.8. *We may move P_0 and $\tilde{P}_0$ as we please within A, without changing the topological configuration of K, $\tilde{K}$, and the constraint points, so long as the following two requirements are satisfied:*

- *We must not change which of the cases of Figure 19 occurs.*
- *Each of P_0 and $\tilde{P}_0$ must remain in the same respective connected component of $A \setminus \cup\{\text{grid lines}\}$.*

During the eventual induction step, it will often be desirable to move the points P_0 and $\tilde{P}_0$. By Observation 6.8 we may do so, within limits, without affecting any relevant aspects of the situation. It will also be useful to note the following:

Observation 6.9. *The points P_0 and $\tilde{P}_0$ lie in different connected components of $A \setminus \cup\{\text{grid lines}\}$, unless $A = A \setminus \cup\{\text{grid lines}\}$.*

This is by our construction of A: if Observation 6.9 fails, then necessarily A meets all three vertical grid lines, thus $z_1 \in a$, contradicting our running assumptions.

Next, recall that we had latitude in choosing the adjacency box A of $p_0, \tilde{p}_0$. With this in mind, we make the following observation:

Observation 6.10. *We may replace A by any topological rectangle contained in A, having sides "parallel to" those of A in the natural sense, so long as the interior of this new rectangle continues to contain P_0 and $\tilde{P}_0$. This replacement preserves the germane features of A in that every argument we have made in this proof so far continues to work under this replacement.*

We now apply these observations to describe how to complete the proof in a crucial case:

Claim 6.11. *Suppose that γ meets only a single connected component of the set $A \setminus \cup\{\text{grid lines}\}$, and furthermore that this component contains a corner of A. Then we may reduce to Claim 6.7, completing the proof of Lemma 1.2.*

Proof. First note that $\gamma \cap A$ has only a single connected component, because γ is "strictly increasing" in $\mathbb{T}$, thus also in the single connected component of $A \setminus \cup\{\text{grid lines}\}$ which γ meets. This also implies that if the component of $A \setminus \cup\{\text{grid lines}\}$ which meets γ contains a corner of A, then it must contain either the upper-left corner $A_{\nwarrow}$ of A, or the lower-right corner $A_{\searrow}$ of A, or both of these. Suppose it contains the upper-left corner. The argument will be the same if it contains the lower-right corner. A potential drawing of the situation is depicted in Figure 20.

Then it is clear that within the constraints described in Observation 6.8 it is possible to move P_0 and $\tilde{P}_0$ if necessary so that both lie to the right of $(x_2, \tilde{x}_2)$ and below $(x_1, \tilde{x}_1)$, and then it is clear how to choose A^* our replacement rectangle for A. This completes the proof of Claim 6.11 by Observation 6.10. □

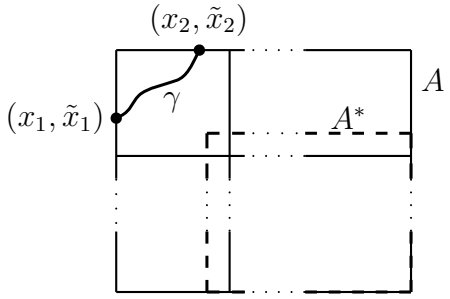

FIGURE 20. **Moving P_0 and $\tilde{P}_0$ to find a replacement for A not meeting γ.** Here $(x_1, \tilde{x}_1)$ is the point in $\mathbb{T}$ where γ enters A, and $(x_2, \tilde{x}_2)$ is the point where γ exits A.

6.7. **Restricting the possibilities further.** Let $p_0, \tilde{p}_0$ be doubly adjacent, with short adjacency arcs a_0 and $\tilde{a}_0$. The unoriented union $a_0 \cup \tilde{a}_0$ is an unoriented Jordan curve. The orientations on a_0 and $\tilde{a}_0$ may or may not agree, and may or may not induce the positive orientation on $a_0 \cup \tilde{a}_0$. Let U be the open Jordan domain bounded by $a_0 \cup \tilde{a}_0$. Then U is called the *adjacency domain* of $p_0, \tilde{p}_0$. We make the following observation:

Observation 6.12. *There exist at least two distinct pairs of doubly adjacent points in $\partial K \cap \partial \tilde{K}$ whose adjacency domains are contained in $\tilde{K}$.*

This is easy to show by arguments similar to those given in the proof of Lemma 3.2. Then we get the following as an immediate corollary:

Observation 6.13. *There exist at least two distinct pairs of doubly adjacent points in $\partial K \cap \partial \tilde{K}$, so that if $p_0, \tilde{p}_0$ is such a pair, then their short adjacency arc in ∂K is $a_0 = [p_0 \to \tilde{p}_0]_{\partial K}$.*

We may restate Observation 6.13 in the following way:

Observation 6.14. *There exist at least two distinct pairs of doubly adjacent points in $\partial K \cap \partial \tilde{K}$, so that if $P_0, \tilde{P}_0 \in \mathbb{T}$ parametrize one of these pairs, then P_0 lies to the left of $\tilde{P}_0$ in their adjacency box A.*

Thus without loss of generality, for the remainder of the proof, we restrict our attention to the arrangements in Figures 19a, 19b, ignoring the possibilities of Figures 19c, 19d.

6.8. **Completing the proof if a constraint lattice point lies in the adjacency box.**

Claim 6.15. *Suppose that A contains a constraint lattice point. Then we may move P_0 and $\tilde{P}_0$ around in such a way that we get $w(\gamma) \geq 0$, completing the proof of Lemma 1.2.*

Proof. The following will be useful to keep in mind:

Observation 6.16. *The curve γ cannot cross grid lines, except at constraint lattice points.*

We prove Claim 6.15 in four cases:

Case 1. The arrangement in Figure 19a occurs, and A does not meet the bottom/top grid line of $\mathbb{T}$.

It is not hard to see that then P_0 and $\tilde{P}_0$ are on different sides of γ in our drawing of $\mathbb{T}$, and furthermore that P_0 lies above γ and $\tilde{P}_0$ below it. Then, arguing straightforwardly as in the proof of Claim 6.7, Case 1, we get $w(\gamma) = w(\gamma') + 1$.

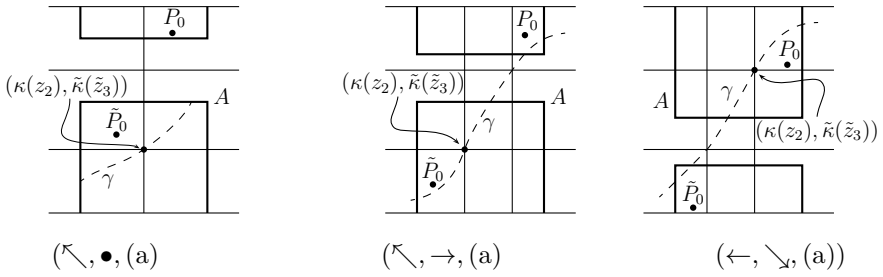

FIGURE 21. **The three possibilities for A when A contains a constraint lattice point and meets the bottom/top grid line, and Figure 19a occurs.**

For the remaining cases, the following will be the key observation:

Observation 6.17. *Suppose that P_0 lies in a connected component of $A \setminus \cup\{\text{grid lines}\}$ through which γ passes. Then we may decide whether P_0 lies above or below γ in our drawing of $\mathbb{T}$, in the sense that we may move P_0 within the constraints given in Observation 6.8 to arrange either situation. The same is true for $\tilde{P}_0$.*

Case 2. The arrangement in Figure 19a occurs, and A crosses the bottom/top grid line of $\mathbb{T}$.

We argue similarly to the proof of Claim 6.7, Case 2. In this case it can always be arranged that P_0 lies below γ and that $\tilde{P}_0$ lies above it. There are three cases to check, and in each it is clear how to proceed. The cases are shown in Figure 21. Again we get $w(\gamma) = w(\gamma') + 1$.

Case 3. The arrangement in Figure 19b occurs, and A does not meet the bottom/top grid line of $\mathbb{T}$.

As per our usual arguments, we have $\omega(\partial\tilde{K}, z_1) = \omega(\partial\tilde{K}', z_1')$ and $\omega(\partial K, \tilde{z}_1) = \omega(\partial K', \tilde{z}_1')$. Thus we will be done if we can argue that we may arrange so that P_0 and $\tilde{P}_0$ lie on the same side of γ in our drawing of $\mathbb{T}$. There are five cases to check, and in each it is clear how to proceed. Figure 22 shows each case.

Case 4. The arrangement in Figure 19b occurs, and A crosses the bottom/top grid line of $\mathbb{T}$.

In this case we have that $\omega(\partial K, \tilde{z}_1) = \omega(\partial K', \tilde{z}_1')$ as per Observation 6.6, but unfortunately $\omega(\partial\tilde{K}, z_1) = \omega(\partial\tilde{K}', z_1') - 1$. Thus we will be done if we can argue that we may arrange so that P_0 lies above γ, and $\tilde{P}_0$ below it, in our drawing of $\mathbb{T}$. There are only three cases to check. Figure 23 shows each. This completes the proof of Claim 6.15. □

6.9. **Completing the proof of Lemma 1.2.** We summarize the situation so far. There are $3 \times 9 = 27$ possibilities for the location of A in $\mathbb{T}$. Most of the cases fall into one of the following three categories. For a given type (s, t) of A, it is quick and easy to check the conditions that define membership in the categories. We also refer the reader back to Figure 18, where each of the 27 cases is drawn.

Category 1. The intersection $A \cap (C_{\swarrow} \cup C_{\bullet} \cup C_{\nearrow})$ is empty.

Then we are done by Claim 6.7, because γ is restricted to lie in $C_{\swarrow} \cup C_{\bullet} \cup C_{\nearrow}$. Next:

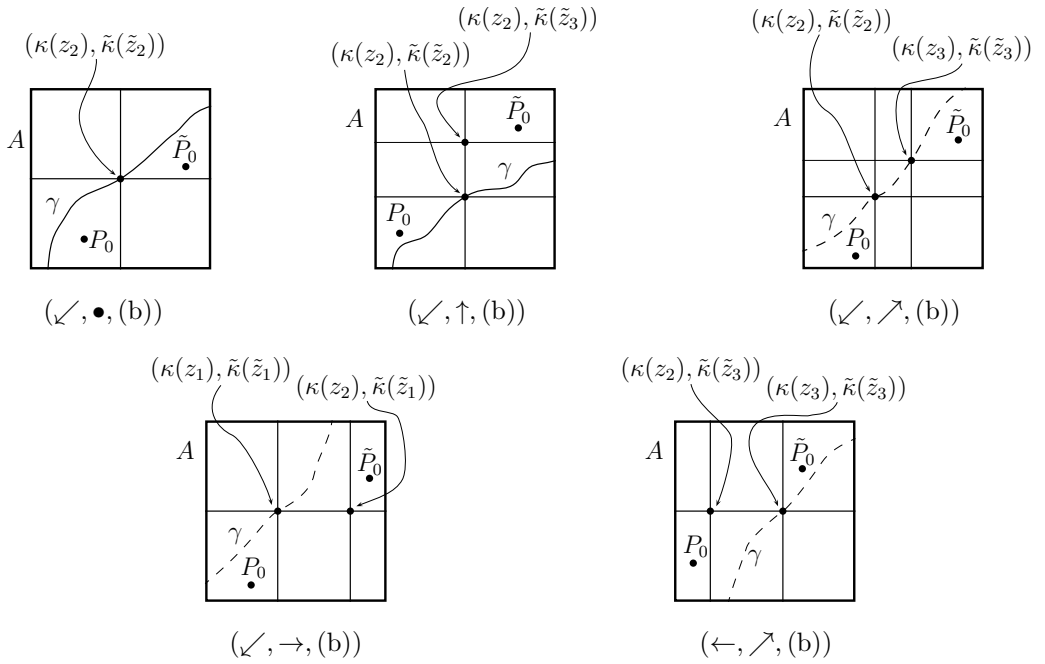

FIGURE 22. **The five possibilities for A when A contains a constraint lattice point and does not meet the bottom/top grid line, and Figure 19b occurs.**

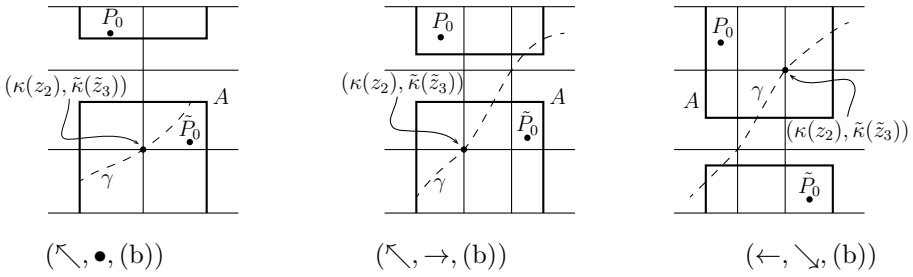

FIGURE 23. **The three possibilities for A when A contains a constraint lattice point and does not meet the bottom/top grid line, and Figure 19b occurs.**

Category 2. The set $A \setminus \cup\{\text{grid lines}\}$ has exactly one connected component lying in $C_{\swarrow} \cup C_{\bullet} \cup C_{\nearrow}$, and this connected component contains a corner of A.

Then we are done by Claim 6.11, again because γ is restricted to lie in $C_{\swarrow} \cup C_{\bullet} \cup C_{\nearrow}$. Finally:

Category 3. The adjacency box A contains a constraint lattice point.

This is exactly handled by Claim 6.15.

In Figure 24 we list the 27 possible locations of A, and for each falling into one of these three categories, we indicate which.

Case $(\leftarrow, \downarrow)$ is easily handled in a manner similar to the proof of Claim 6.11. If case $(\leftarrow, \rightarrow)$ occurs, then our running assumption that P_0 lies to the left of $\tilde{P}_0$ in A implies that $w(\gamma) = w(\gamma') + 1$ by Lemma 5.3 as usual.

r	s	Category
$\nwarrow$	$\uparrow$	1
$\nwarrow$	$\nearrow$	3
$\nwarrow$	$\rightarrow$	2
$\nwarrow$	$\searrow$	3
$\nwarrow$	$\downarrow$	3
$\nwarrow$	$\swarrow$	3
$\nwarrow$	$\leftarrow$	
$\nwarrow$	$\nwarrow$	1
$\nwarrow$	$\bullet$	2

r	s	Category
$\leftarrow$	$\uparrow$	3
$\leftarrow$	$\nearrow$	2
$\leftarrow$	$\rightarrow$	
$\leftarrow$	$\searrow$	2
$\leftarrow$	$\downarrow$	
$\leftarrow$	$\swarrow$	3
$\leftarrow$	$\leftarrow$	1
$\leftarrow$	$\nwarrow$	1
$\leftarrow$	$\bullet$	3

r	s	Category
$\swarrow$	$\uparrow$	2
$\swarrow$	$\nearrow$	2
$\swarrow$	$\rightarrow$	2
$\swarrow$	$\searrow$	3
$\swarrow$	$\downarrow$	3
$\swarrow$	$\swarrow$	3
$\swarrow$	$\leftarrow$	3
$\swarrow$	$\nwarrow$	3
$\swarrow$	$\bullet$	2

FIGURE 24. **The cases to check for Lemma 1.2.**

We have no way to deal with case $(\nwarrow, \leftarrow)$ directly. However, recall from Observation 6.14 that we had two choices for $P_0, \tilde{P}_0$ for which every step of the proof until this point go through. Because the adjacency arc $\tilde{a}_0$ contains two constraint points $\tilde{z}_i$ if case $(\nwarrow, \leftarrow)$ occurs, it can occur for only one of these two choices of $P_0, \tilde{P}_0$, so we do not need to handle this case directly. This completes the proof of Lemma 1.2. □

REFERENCES

[And70] E. M. Andreev, *Convex polyhedra of finite volume in Lobačevskiĭ space*, Mat. Sb. (N.S.) **83 (125)** (1970), 256–260 (Russian). MR0273510 (42 #8388)

[FM12] Benson Farb and Dan Margalit, *A primer on mapping class groups*, Princeton Mathematical Series, vol. 49, Princeton University Press, Princeton, NJ, 2012. MR2850125

[HS93] Zheng-Xu He and Oded Schramm, *Fixed points, Koebe uniformization and circle packings*, Ann. of Math. (2) **137** (1993), no. 2, 369–406, DOI 10.2307/2946541. MR1207210 (96b:30015)

[Koe36] Paul Koebe, *Kontaktprobleme der Konformen Abbildung*, Ber. Verh. Sächs. Akad. Wiss. Leipzig **88** (1936), 141–164 (German).

[Mer12] Sergei Merenkov, *Planar relative Schottky sets and quasisymmetric maps*, Proc. Lond. Math. Soc. (3) **104** (2012), no. 3, 455–485, DOI 10.1112/plms/pdr038. MR2900233

[Mis12] Andrey Mishchenko, *Rigidity of thin disk configurations*, Ph.D. thesis, University of Michigan, 2012. Available online at `http://hdl.handle.net/2027.42/95930`.

[Mis13] Andrey M. Mishchenko, *Rigidity of thin disk configurations, via fixed-point index* (2013). (submitted), `arXiv:1302.2380 [math.MG]`.

[Roh11] Steffen Rohde, *Oded Schramm: from circle packing to SLE*, Ann. Probab. **39** (2011), no. 5, 1621–1667, DOI 10.1007/978-1-4419-9675-6_1. MR2884870

[Sac94] Horst Sachs, *Coin graphs, polyhedra, and conformal mapping*, Discrete Math. **134** (1994), no. 1-3, 133–138, DOI 10.1016/0012-365X(93)E0068-F. Algebraic and topological methods in graph theory (Lake Bled, 1991). MR1303402 (95j:52020)

[Sch91] Oded Schramm, *Rigidity of infinite (circle) packings*, J. Amer. Math. Soc. **4** (1991), no. 1, 127–149, DOI 10.2307/2939257. MR1076089 (91k:52027)

[Ste05] Kenneth Stephenson, *Introduction to circle packing: the theory of discrete analytic functions*, Cambridge University Press, Cambridge, 2005. MR2131318 (2006a:52022)

[Str51] Kurt Strebel, *Über das Kreisnormierungsproblem der konformen Abbildung*, Ann. Acad. Sci. Fennicae. Ser. A. I. Math.-Phys. **1951** (1951), no. 101, 22 (German). MR0051934 (14,549j)

[Thu80] William Thurston, *The Geometry and Topology of Three-Manifolds*, Princeton University, 1980, unpublished lecture notes, version 1.1. At the time of writing, these notes were available online at `http://library.msri.org/books/gt3m/`.

E-mail address: `misHchea@umich.edu`